Atoms and Light

14

This chapter describes some of the biologically important properties of infrared, visible, and ultraviolet light. X rays are discussed in Chaps. 15 and 16. A brief discussion of geometrical optics accompanies the description of image formation in the eye and errors of refraction.

Section 14.1 considers the particle properties of light (photons), while Sect. 14.2 looks at the wave properties of electrons. Photons can be emitted or absorbed when single atoms change energy levels, and they have certain frequencies characteristic of the atom, as described in Sect. 14.3. Molecules have additional energy levels shown in Sect. 14.4. Biological examples include spectrophotometry, photodissociation, immunofluorescence, infrared spectroscopy, and Raman scattering. There is an extensive literature about these; the discussion here is quite brief.

Section 14.5 describes the scattering and absorption of radiation, processes that are important in the rest of this chapter and in Chaps. 15–17. The probability of scattering or absorption is measured by the cross section, which is also introduced here. Photons may scatter many times in a substance without being absorbed. This leads to the concept of turbid media such as milk or clouds. In some cases the process can be modeled accurately with the diffusion approximation developed in Sect. 14.6. Biological examples of infrared scattering (including Raman scattering) are described in Sect. 14.7

Photons can be absorbed and emitted by some substances in a continuous range of frequencies or wavelengths. This happens when many atoms interact with each other and blur the energy levels, as in liquids and solids. This leads to the concept of thermal radiation described in Sect. 14.8. Examples of thermal radiation are infrared radiation by the skin and ultraviolet radiation by the sun. The former is discussed in Sect. 14.9.

Blue and ultraviolet light are used for therapy, as described in Sect. 14.10. They can also be harmful, particularly to skin and eyes.

Lasers are used to heat tissue, often rapidly enough to do surgery as water in the tissue suddenly boils. Models of this process include the bioheat equation that is developed in Sect. 14.11.

Section 14.12 describes the problem of radiometry: measuring radiation. All of the important quantities are defined, and the corresponding photometric and actinometric quantities are also introduced.

Section 14.13 describes how the eye focuses an image on the retina and the correction of simple errors of refraction. A final example of the photon nature of light is given in Sect. 14.14: the statistical limit to dark-adapted vision—shot noise—which is important when the eye is operating in its most sensitive mode.

We can only provide a brief introduction to the role optics and light play in biology. For more details with many fascinating examples, see Johnsen (2011).

14.1 The Nature of Light: Waves and Photons

Light travels in a vacuum with a velocity $c = 3 \times 10^8\,\mathrm{m\,s^{-1}}$ (to an accuracy of 0.07 %). When light travels through matter, its speed is less than this and is given by

$$c_n = \frac{c}{n}, \tag{14.1}$$

where n is the *index of refraction* of the substance. The value of the index of refraction depends on both the composition of the substance and the color of the light.

A controversy over the nature of light existed for centuries. Sir Isaac Newton explained many properties of light with a particle model in the seventeenth century. In the early nineteenth century, Thomas Young performed some interference experiments that could be explained only by assuming that light is a wave. By the end of the nineteenth century, nearly all known properties of light, including many of

R. K. Hobbie, B. J. Roth, *Intermediate Physics for Medicine and Biology*,
DOI 10.1007/978-3-319-12682-1_14,

its interactions with matter, could be explained by assuming that light consists of an electromagnetic wave. By an electromagnetic wave, we mean that

1. Light can be produced by accelerating an electric charge.
2. Light has an electric and a magnetic field associated with it; the force that the light exerts on a charged particle is given by Eq. 8.2, $\mathbf{F} = q(\mathbf{E} + \mathbf{v} \times \mathbf{B})$. The force due to the magnetic field is usually very small.
3. The velocity of light traveling in a vacuum is given by electromagnetic theory as $c = 1/\sqrt{\epsilon_0 \mu_0}$, where parameters ϵ_0 and μ_0 are measured in the laboratory for "ordinary" electric and magnetic fields.

In the early twentieth century, light was discovered to have *both* particle properties and electromagnetic wave properties at the same time. This rather disconcerting discovery was followed in a few years by the discovery that matter, which had been thought to consist of particles, also has wave properties.

A traveling wave of light can be described by a function of the form $f(x - c_n t)$, which represents a disturbance traveling along the x axis in the positive direction. If the wave is sinusoidal, then the period T, frequency ν,[1] and wavelength λ are related by

$$\nu = \frac{1}{T}, \qquad c_n = \lambda \nu. \tag{14.2}$$

As light moves from one medium into another where it travels with a different speed, the frequency remains the same. The wavelength changes as the speed changes.

Each particle of light or *photon* has energy E. The energy of each photon (a "particle" concept) is related to its frequency (a "wave" concept) by

$$E = h\nu = \frac{hc_n}{\lambda}. \tag{14.3}$$

The proportionality constant h is called *Planck's constant*. It has the numerical value[2]

$$h = 6.63 \times 10^{-34}\,\mathrm{J\,s} = 4.14 \times 10^{-15}\,\mathrm{eV\,s}. \tag{14.4}$$

We use the number "h stroke" or "h bar":

$$\hbar = \frac{h}{2\pi} = 1.05 \times 10^{-34}\mathrm{J\,s} = 0.66 \times 10^{-15}\,\mathrm{eV\,s}. \tag{14.5}$$

In terms of the angular frequency $\omega = 2\pi\nu$,

$$E = \hbar\omega. \tag{14.6}$$

[1] We used f for frequency in earlier chapters because this is customary when discussing noise. Here we adopt ν for frequency, the notation most often used in atomic physics.

[2] The electron volt (eV) is a unit of energy. $1\mathrm{eV} = 1.6 \times 10^{-19}$ J. It is the energy acquired by an electron that moves through a potential difference of 1 V.

Table 14.1 The regions of the electromagnetic spectrum and their boundaries

Name	Wavelength	Frequency (Hz)	Energy (eV)
Radio waves			
	1 m	300×10^6	1.24×10^{-6}
Microwaves			
	1 mm	300×10^9	1.24×10^{-3}
Extreme infrared			
	15 μm	20×10^{12}	0.083
Far infrared			
	6 μm	50×10^{12}	0.207
Middle infrared			
	3 μm	100×10^{12}	0.414
Near infrared			
	750 nm	400×10^{12}	1.65
Visible			
	400 nm	750×10^{12}	3.11
Ultraviolet			
	12 nm	24×10^{15}	100
X rays, γ rays			

Table 14.2 The visible electromagnetic spectrum

Color	Wavelength (nm)	Frequency (THz)	Energy (eV)
	750	400	1.65
Red			
	610	490	2.03
Orange			
	590	510	2.10
Yellow			
	570	530	2.17
Green			
	500	600	2.48
Blue			
	450	670	2.76
Violet			
	400	750	3.11

The electromagnetic spectrum includes radio waves, microwaves, infrared, visible, and ultraviolet light, x rays, and γ (gamma) rays. Table 14.1 shows the wavelengths that separate these arbitrary regions, together with the frequencies and the energies of the photons. Visible-light photons have an energy of a few electron volts. X rays are 10^4–10^7 times more energetic, while γ rays, which come from atomic nuclei, are often even more energetic but may have energies overlapping x-ray energies. The only difference between x rays and γ rays is their source.

The property of light that we associate with color is the frequency or the energy of each photon. Visible light covers a narrow range of frequencies, about an octave (a factor of 2). Table 14.2 shows the wavelengths and frequencies dividing the colors of the visible spectrum. The frequencies are in the 400–750 THz range.

Most of the effects discussed in this chapter, particularly those dealing with emission and absorption, can be explained by assuming that light is made up of photons. Phenomena

such as interference, diffraction, and polarization require the wave theory.

14.2 Electron Waves and Particles: The Electron Microscope

Like light, matter can have both wave and particle properties. The French physicist, Louis de Broglie, derived a quantum mechanical relationship between a particle's momentum p and wavelength:

$$\lambda = \frac{h}{p} \tag{14.7}$$

(Eisberg and Resnick 1985). For example, a 100-eV electron has a speed of $5.9 \times 10^6\ \mathrm{m\,s^{-1}}$ (about 2 % the speed of light), a momentum of $5.4 \times 10^{-24}\ \mathrm{kg\,m\,s^{-1}}$, and a wavelength of 12 nm.

The electron microscope takes advantage of the short wavelength of electrons to produce exquisite pictures of very small objects. Diffraction limits the spatial resolution of an image to about a wavelength. For a visible light microscope, this resolution is on the order of 500 nm (Table 14.2). For the electron microscope, however, the wavelength of the electron limits the resolution. A typical electron energy used for imaging is about 100 keV, implying a wavelength much smaller than an atom (however, practical limitations often limit the resolution to about 1 nm). Table 1.2 shows that viruses appear as blurry smears in a light microscope, but can be resolved with considerable detail in an electron microscope. In 1986, Ernst Ruska shared the Nobel Prize in Physics "for his fundamental work in electron optics, and for the design of the first electron microscope."

Electron microscopes come in two types. In a transmission electron microscope (TEM), electrons pass through a thin sample. In a scanning electron microscope (SEM), a fine beam of electrons is raster scanned across the sample, and secondary electrons emitted by the surface are imaged. In both cases, the image is formed in vacuum and the electron beam is focused using a magnetic lens.

14.3 Atomic Energy Levels and Atomic Spectra

The simplest system that can emit or absorb light is an isolated atom. An atom is isolated if it is in a monatomic gas. In addition to translational kinetic energy, isolated atoms have specific discrete internal energies, called *energy levels*. An atom can change from one energy level to another by emitting or absorbing a photon with an energy equal to the energy difference between the levels. Let the energy levels be labeled by $i = 1, 2, 3, \ldots$, with the energy of the ith state being E_i. There is a lowest possible internal energy for the atom; when the atom is in this state, no further energy loss can take place. If E_i is greater than the lowest energy, then the atom can lose energy by emitting a photon of energy $E_i - E_f$ and exist in a lower energy state E_f (Fig. 14.1).

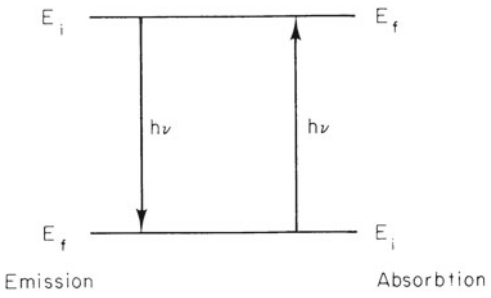

Fig. 14.1 A system can change from one energy to another by emitting or absorbing a photon. The photon has an energy equal to the difference in energies of the two levels

It is possible, using techniques of quantum mechanics, to calculate the energies of the levels with reasonable accuracy (and in some cases with spectacular accuracy). For our purposes, we need to only recognize that energy levels exist and know their approximate values. You may be familiar with the model of the hydrogen atom developed by Niels Bohr, in which the energy of the nth level is given by

$$E_n = -\left(\frac{1}{4\pi\epsilon_0}\right)^2 \frac{m_e e^4}{2\hbar^2 n^2}, \quad n = 1, 2, 3, \ldots. \tag{14.8}$$

The energy is in joules when the electron mass m_e is in kilograms, the electronic charge e is in coulombs, and $\hbar$ is in J s. The Coulomb's law constant $1/4\pi\epsilon_0$ is given in Eq. 6.2. Dividing the energy in joules by e gives the energy in electron volts:

$$E_n = -\frac{13.6}{n^2} \quad \text{(in eV)}. \tag{14.9}$$

The energy-level diagram in Fig. 14.2 shows these energies and some transitions between them. In other cases, the energy depends not only on the integer $n = 1, 2, 3, 4, \ldots$, but on additional quantum numbers as well.

Figure 14.3 plots the spectrum for hydrogen versus wavelength, along with some of the energy levels of hydrogen. Letters $a, b, c, \ldots$ mark lines in the spectrum and the associated transitions.

In general, the internal energy of an atom depends on the values of five quantum numbers for each electron in the atom. The quantum numbers are

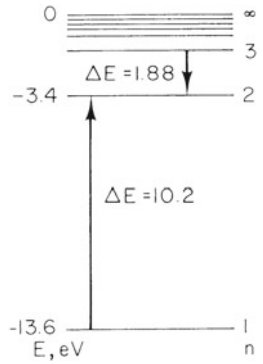

Fig. 14.2 Energy levels in a hydrogen atom. Transitions are shown corresponding to the emission and absorption of light

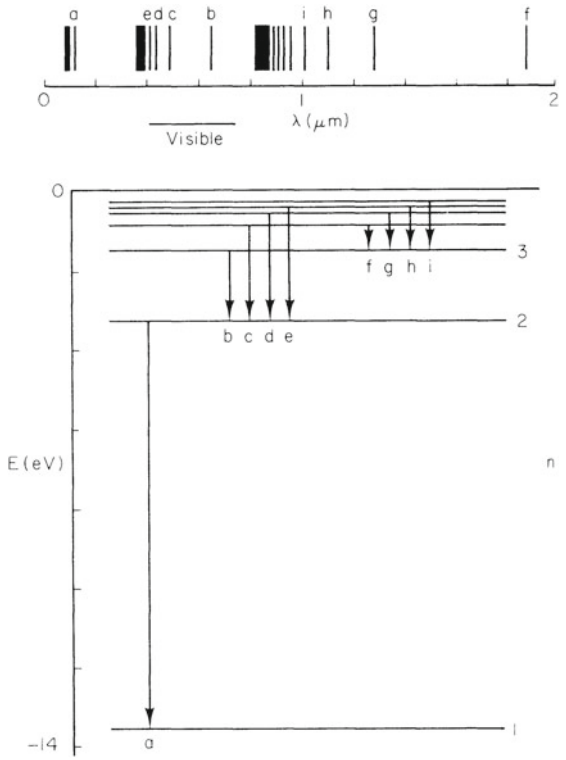

Fig. 14.3 The spectrum for hydrogen plotted versus wavelength and the energy levels for hydrogen. Some spectral lines and the corresponding transitions have been labeled

$n = 1, 2, 3, \ldots$	the principal quantum number
$l = 0, 1, 2, \ldots, n-1$	the orbital angular momentum quantum number
$s = \frac{1}{2}$	the spin quantum number
$m_l = -l, -(l-1), \ldots, l-1, l$	"z component" of the orbital angular momentum
$m_s = -\frac{1}{2}, \frac{1}{2}$	"z component" of the spin.

Sometimes the last two quantum numbers, m_l and m_s, are replaced by two other quantum numbers, j and m_j. The allowed values of j and m_j are

$j = l - \frac{1}{2}$ or $l + \frac{1}{2}$ except that $j = \frac{1}{2}$ when $l = 0$	total angular momentum quantum number
$m_j = -j, -(j-1), \ldots, j-1, j$	"z component" of total angular momentum

Whether one uses m_l and m_s or j and m_j, each electron is described by five quantum numbers, one of which is always $\frac{1}{2}$. There are four quantum numbers that can change, corresponding to the three space degrees of freedom and the spin associated with m_s. The internal energy of the atom is the sum of the kinetic and potential energies of each electron. The energy of each electron depends on the values of its quantum numbers. It is influenced by the electric field generated by the nucleus and all the other electrons. There are also magnetic interactions between electrons and between each electron and the nucleus, because the moving charges generate magnetic fields.

No two electrons in an atom can have the same values for all their quantum numbers, a fact known as the *Pauli exclusion principle.*

The *ionization energy* is the smallest amount of energy required to remove an electron from the atom when the atom is in its ground state. For hydrogen the ionization energy is 13.6 eV. In contrast, it takes only 5.1 eV to remove the least tightly bound electron from a sodium atom.

An atom can receive energy from an external source, such as a collision with another atom or some other particle. It can also absorb a photon of the proper energy. Absorbing just the right amount of energy allows one of its electrons to move to a higher energy level, as long as that level is not already occupied. The atom can then get rid of this excess energy by radiating a photon, with the excited electron falling to an unoccupied state with lower energy. This change is usually consistent with the following *selection rules*, which can be derived using quantum mechanics:

$$\Delta l = 1, \quad \Delta j = 0, \pm 1. \tag{14.10}$$

14.4 Molecular Energy Levels

In addition to internal energy, an atom can have kinetic energy of translation with three degrees of freedom. The translational kinetic energy is also quantized, but as long as the atom is not confined to a very small volume, the levels are so closely spaced that the translational kinetic energy can be regarded as continuous.

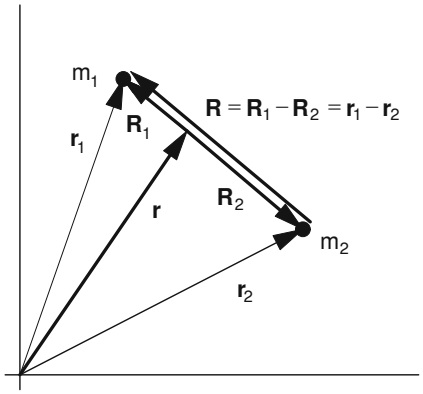

Fig. 14.4 A diatomic molecule. Vectors $\mathbf{r}_1$ and $\mathbf{r}_2$ are the positions of the atoms measured in the laboratory. Vectors $\mathbf{R}_1$ and $\mathbf{R}_2$ are coordinates in the center-of-mass system. Vector $\mathbf{r}$ is the position of the center of mass

Two atoms together have six degrees of translational freedom, because each can move in three-dimensional space. However, if the atoms are bound together, their motions are not independent One can speak of the three degrees of freedom for translation of the molecule as a whole (center-of-mass motion) and also the vector displacement of one atom from the other. This is shown in Fig. 14.4. Vector $\mathbf{r}$ locates the center of mass of the two atoms. It is located at a point such that $m_1\mathbf{R}_1 = -m_2\mathbf{R}_2$.

Consider two particles of mass m_1 and m_2. Their positions with respect to some fixed origin are $\mathbf{r}_1$ and $\mathbf{r}_2$. The velocity of each particle is $\mathbf{v}_i = d\mathbf{r}_i/dt$. The kinetic energy of the ith particle is $T_i = m_i(\mathbf{v}_i \cdot \mathbf{v}_i)/2$. Define the center of mass by

$$\mathbf{r} = \frac{m_1\mathbf{r}_1 + m_2\mathbf{r}_2}{m_1 + m_2}$$

and the vectors from the center of mass to each particle by

$$\mathbf{R}_1 = \mathbf{r}_1 - \mathbf{r} = \frac{m_2(\mathbf{r}_1 - \mathbf{r}_2)}{m_1 + m_2} = \frac{m_2\mathbf{R}}{m_1 + m_2},$$
$$\mathbf{R}_2 = \frac{-m_1\mathbf{R}}{m_1 + m_2}.$$

The total kinetic energy is $T = m_1(\mathbf{v}_1 \cdot \mathbf{v}_1)/2 + m_2(\mathbf{v}_2 \cdot \mathbf{v}_2)/2$. Since $\mathbf{v}_i = \mathbf{v} + \mathbf{V}_i$, we have

$$2T = (m_1 + m_2)(\mathbf{v} \cdot \mathbf{v}) + m_1(\mathbf{V}_1 \cdot \mathbf{V}_1) + m_2(\mathbf{V}_2 \cdot \mathbf{V}_2) + 2\mathbf{v} \cdot (m_1\mathbf{V}_1 + m_2\mathbf{V}_2).$$

The last term vanishes because $m_1\mathbf{R}_1 + m_2\mathbf{R}_2 = 0$. Consider the second term. Differentiating $\mathbf{R}_1 = m_2\mathbf{R}/(m_1 + m_2)$ shows that

$$\mathbf{V}_1 \cdot \mathbf{V}_1 = \left(\frac{m_2}{m_1 + m_2}\right)^2 V^2,$$
$$\mathbf{V}_2 \cdot \mathbf{V}_2 = \left(\frac{m_1}{m_1 + m_2}\right)^2 V^2.$$

Therefore,

$$T = \frac{(m_1 + m_2)v^2}{2} + \frac{1}{2}\frac{m_1 m_2}{m_1 + m_2}V^2.$$

The first term is the kinetic energy of a point mass $m_1 + m_2$ traveling at the speed of the center of mass. The second is the kinetic energy of a particle having the *reduced mass* $m_1m_2/(m_1 + m_2)$ and the speed of relative motion of the two particles, $V = |\mathbf{V}| = |d\mathbf{R}/dt|$. If $\mathbf{R}$ changes magnitude, the particles are *vibrating*. If $\mathbf{R}$ has a fixed magnitude, the molecule can *rotate*. If the molecule is rotating in some plane with angular velocity ω, then

$$\frac{1}{2}\frac{m_1 m_2}{m_1 + m_2}V^2 = \frac{1}{2}\frac{m_1 m_2}{m_1 + m_2}R^2\omega^2 = \frac{1}{2}I\omega^2.$$

The quantity $I = \left[m_1m_2/(m_1 + m_2)\right]R^2 = m_1R_1^2 + m_2R_2^2$ is the *moment of inertia* of the two objects (Serway and Jewett 2013, p. 312 and 328). In this case the angular momentum about the center of mass is

$$L = R_1(m_1v_1) + R_2(m_2v_2) = m_1R_1^2\omega + m_2R_2^2\omega = I\omega.$$

These two equations can be combined to give the rotational kinetic energy in terms of the angular momentum about the center of mass:

$$T = \frac{L^2}{2I}.$$

Quantum mechanically, the angular momentum cannot take on any arbitrary value. The square of the angular momentum is restricted to the values

$$L^2 = r(r + 1)\hbar^2, \qquad r = 0, 1, 2, \ldots.$$

Since there is no potential energy, the total energy of rotation of the molecule is

$$E_r = \frac{r(r + 1)\hbar^2}{2I}, \qquad r = 0, 1, 2, \ldots. \tag{14.11}$$

The spacing of the rotational levels is shown in Fig. 14.5. A detailed calculation using quantum mechanics shows that when a photon is emitted or absorbed, r must change by ± 1. Therefore the photon energy is

$$\Delta E_r = E_r - E_{r-1} = \frac{\hbar^2}{I}r, \qquad r = 1, 2, \ldots. \tag{14.12}$$

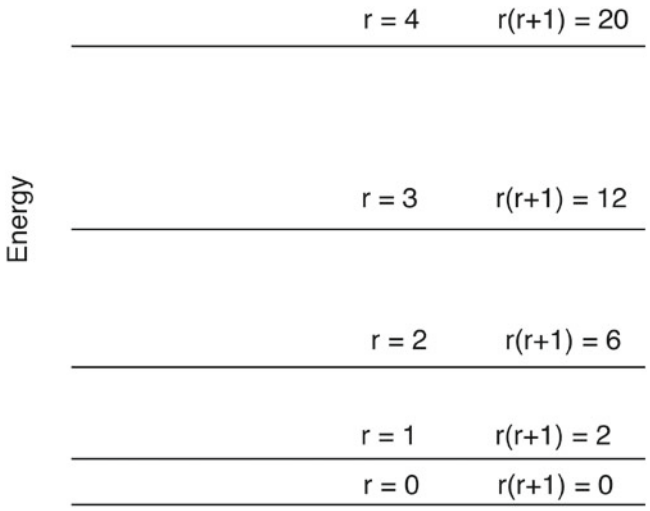

Fig. 14.5 Energy levels of a rotating molecule

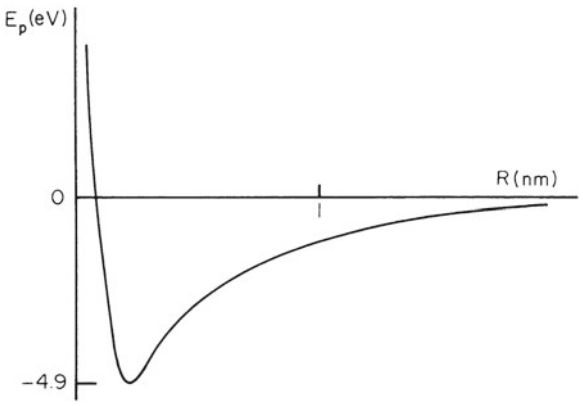

Fig. 14.6 The potential energy of a sodium ion and a chloride ion as a function of their nuclear separation

The problems at the end of the chapter show that these photons have low energies, so that rotational spectra lie in the far-infrared region (far meaning far from the visible region, i.e., very long wavelengths).

The other possibility is that the atoms in the molecule vibrate back and forth along the line joining their centers. If two masses have an equilibrium position a certain distance apart, work must done either to push them closer together or to pull them farther apart. In either case, the potential energy is increased. At the equilibrium separation the potential energy is a minimum. Figure 14.6 shows the potential energy E_p of a sodium ion and a chloride ion as a function of their separation. The potential has a minimum at a separation R_0 of about 0.2 nm. The simplest function that has a minimum is a parabola. A parabola can be used to approximate the minimum in Fig. 14.6: $E_p(R) = \frac{1}{2}k(R - R_0)^2$. Since (see Sect. 6.4) $dE_p = -F dr$, the force is $F = -dE_p/dR = -k(R - R_0)$, which is the linear approximation to the force between the two ions. The force is attractive if $R > R_0$ and repulsive if $R < R_0$.

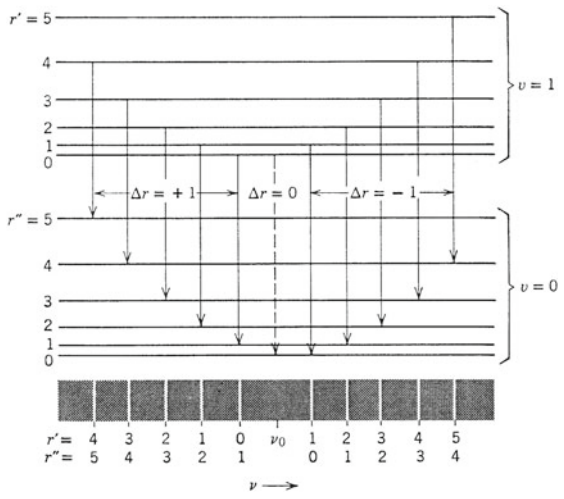

Fig. 14.7 Transitions for vibrational–rotational spectra. (Source: Eisberg and Resnick 1985. Copyright ©1985 John Wiley & Sons. Reproduced by permission of John Wiley & Sons, Inc.)

A mass subject to a linear restoring force is called a *harmonic oscillator* (Appendix F). A mass m subject to a linear restoring force $-kx$ oscillates with an angular frequency $\omega^2 = k/m$. Classically, the energy of the oscillating mass depends on the amplitude of the motion and can have any value. Quantum mechanically, it is restricted to values

$$E_v = \hbar\omega\left(v + \tfrac{1}{2}\right), \qquad v = 0, 1, 2, \ldots. \tag{14.13}$$

This is the total energy, including both kinetic and potential energy. The levels are spaced equally by an amount $\hbar\omega$. The spacing is usually greater than that for rotational levels, often in the infrared. The transitions that give rise to the emission or absorption of photons require a change in the rotational quantum numbers as well as the vibrational ones. The selection rules are

$$\Delta r = \pm 1, \qquad \Delta v = \pm 1. \tag{14.14}$$

Some of these vibrational–rotational transitions are shown in Fig. 14.7.

Finally, there can be transitions involving v, r, and the electronic quantum numbers as well. When the electronic quantum numbers change, the shape of the interatomic potential changes, as shown in Fig. 14.8. The details of molecular spectra are fairly involved and are summarized in many texts. Transitions of biological importance are discussed in Grossweiner (1994, pp. 33–38). If the electron selection rules are satisfied, the transition is fairly rapid (typically 10^{-8}s), a process called *fluorescence*. Sometimes the electron becomes

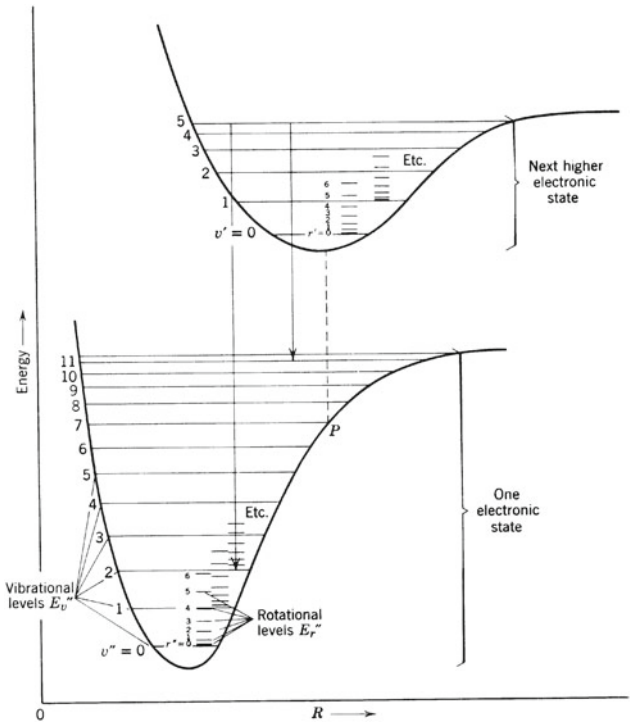

Fig. 14.8 A combination of changes in electronic quantum numbers within an atom and of vibrational and rotational quantum numbers within the molecule. (Source: Eisberg and Resnick 1985. Copyright ©1985 John Wiley & Sons. Reproduced by permission of John Wiley & Sons, Inc)

trapped in a state where it cannot decay according to the electronic selection rules of Eq. 14.10. It may then have a lifetime up to several seconds before decaying, a phenomenon called *phosphorescence*.

14.5 Scattering and Absorption of Radiation; Cross Section

In the absence of interference and diffraction effects, photons in a vacuum travel in a straight line. When they travel through matter they are apparently slowed down, leading to an index of refraction greater than unity; they may also be scattered or absorbed. Visible light does not pass through a building wall, but it does pass through a glass window. The absorption may depend on the frequency or wavelength of the light. The window can be made of colored glass. The light can also be scattered. This leads to the blue of the sky or to the white of clouds. If there is absorption as well as scattering, the clouds may appear gray instead of white. How light is scattered or absorbed in tissue has become very important in biophysics. Infrared light absorption can be used to measure chemical composition of the body. Light is also used for therapy and for laser surgery.

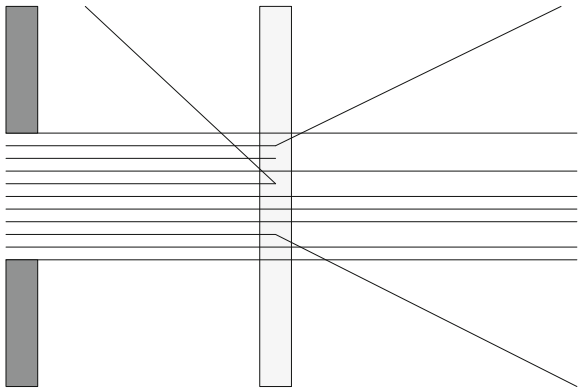

Fig. 14.9 A collimated beam of photons passes from left to right through a thin slice of material. Some photons pass through, some are scattered, and some are absorbed

This section shows how to describe a single interaction of a photon with some substance. The photon can be scattered or absorbed. Section 14.6 develops one technique for calculating what happens when the photon undergoes many scattering events before being absorbed or emerging from the material.

Imagine that we have a distant source of photons that travel in straight lines, and that we collimate the beam (send it through an aperture) so that a nearly parallel beam of photons is available to us. Imagine also that we can see the tracks of the N photons in the beam, as in Fig. 14.9. When a thin sample of material of thickness dz is placed in the beam, a certain number of photons are scattered and a certain number are absorbed. If we repeat the experiment many times, we find that the number of photons scattered fluctuates about an average value that we call dN_s and the number absorbed fluctuates about an average value dN_a. When we vary the thickness of the absorber, we find that if it is sufficiently thin, the average number of photons scattered and absorbed is proportional to the thickness as well as the number of incident photons:

$$dN_s = \mu_s N dz, \qquad dN_a = \mu_a N dz. \tag{14.15}$$

The total number of unscattered photons N changes according to

$$dN = -(dN_s + dN_a) = -N(\mu_s + \mu_a)dz$$

with solution

$$N(z) = N_0 e^{-\mu z} = N_0 e^{-(\mu_s + \mu_a)z}. \tag{14.16}$$

The quantity μ is the *total linear attenuation coefficient*. Quantities μ_s and μ_a are the linear scattering and absorption coefficients. Both depend on the material and the energy

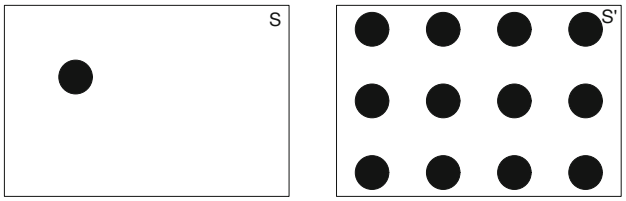

Fig. 14.10 Each circle represents the cross section σ associated with a target entity such as an atom. **a** There is one atom in area S. **b** There are N_T target atoms per unit area in area S'

of the photons. This kind of exponential absorption is known as *Beer's law* or the *Beer–Lambert* law.

The interaction of photons with matter is statistical. The *cross section* σ is an effective area proportional to the probability that an interaction takes place. The interaction takes place with a *target entity*. It is sometimes convenient to define the target to be a single molecule, at other times an atom, and still other times one of the electrons within an atom. We can visualize the meaning of the cross section by considering either a single target entity interacting with a beam of photons or a single photon interacting with a thin foil of targets. Both are shown in Fig. 14.10. For the single target in Fig. 14.10a, consider a beam of N photons passing through the area S with a uniform number per unit area N/S. Let the average number of interactions be $\overline{n}$. The cross section per target entity is defined by saying that the fraction of photons that interact is equal to the fraction of the area occupied by the cross section:

$$\frac{\overline{n}}{N} = \frac{\sigma}{S}. \tag{14.17}$$

We denote the number of photons per unit area by Φ and write Eq. 14.17 as $\overline{n} = \sigma\Phi$. This is the average number of scatterings per target entity or the *probability of interaction per target entity when the beam has Φ photons per unit area*:

$$p = \sigma\Phi. \tag{14.18}$$

Strictly speaking, $\overline{n}$ is dimensionless, σ has the dimensions m^2, and Φ has dimensions m^{-2}. However, it is often helpful to think of $\overline{n}$ as being interactions per target entity and σ as being m^2 per target entity.

Alternatively, imagine sending a beam of photons at the target of area S' shown in Fig. 14.10b. There are N_T target entities per unit area in the path of the beam, each having an associated area σ. The fraction of the photons that interact is again the fraction of the area that is covered:

$$\frac{\overline{n}}{N} = \frac{\sigma S' N_T}{S'} = \sigma N_T. \tag{14.19}$$

This is the *probability that a single photon interacts when there are N_T target entities per unit area*. Note the symmetry with Eq. 14.18. In the first case, there is one target entity and a certain number of photons per unit area. In the second case, there is one photon and a certain number of target entities per unit area.

If a number of mutually exclusive interactions can take place (such as absorption and scattering), we can define a cross section for each kind of interaction. The probabilities and the cross sections add:

$$\sigma_{\mathrm{tot}} = \sum_i \sigma_i. \tag{14.20}$$

The second interpretation we had above can be used to relate the cross section to the attenuation coefficient. The number of target entities per unit area is equal to the number per unit volume times the thickness of the target along the beam. To obtain the number of target atoms per unit volume, recall that 1 mol of atoms contains Avogadro's number N_A atoms. If A is the mass of a target containing 1 mol of atoms and the target has mass density ρ, then volume V has mass ρV and contains $\rho V/A$ mol and $N_A\rho V/A$ atoms. Therefore the number of atoms per unit volume is $N_A\rho/A$, and the number of atoms per unit area is

$$N_T = \frac{N_A\rho}{A}dz. \tag{14.21}$$

The linear coefficients are related to their corresponding cross sections by

$$\begin{aligned} \mu_s &= \frac{N_A\rho}{A}\sigma_s, \\ \mu_a &= \frac{N_A\rho}{A}\sigma_a, \\ \mu &= \frac{N_A\rho}{A}(\sigma_s + \sigma_a) = \frac{N_A\rho}{A}\sigma_{\mathrm{tot}}, \end{aligned} \tag{14.22}$$

where σ_{tot} is the sum of all the interaction cross sections.

Be careful with units! Avogadro's number is 6.022141×10^{23} entities per mole, which is the number in a **gram** atomic weight. For carbon, $A = 12.01 \times 10^{-3}$ kg mol^{-1} and $\rho = 2.0 \times 10^3$ kg m^{-3}. This is discussed further on page 433.

We may wish to know the probability that particles (in this case photons) are scattered in a certain direction. We have to consider the probability that they are scattered into a small solid angle $d\Omega$. In this case, σ is called the *differential scattering cross section* and is often written as

$$\frac{d\sigma}{d\Omega}d\Omega \qquad \text{or} \qquad \sigma(\theta)d\Omega. \tag{14.23}$$

The units of the differential scattering cross section are m^2 sr^{-1}. The differential cross section depends on θ, the angle between the directions of travel of the incident and scattered particles. In a spherical coordinate system in which

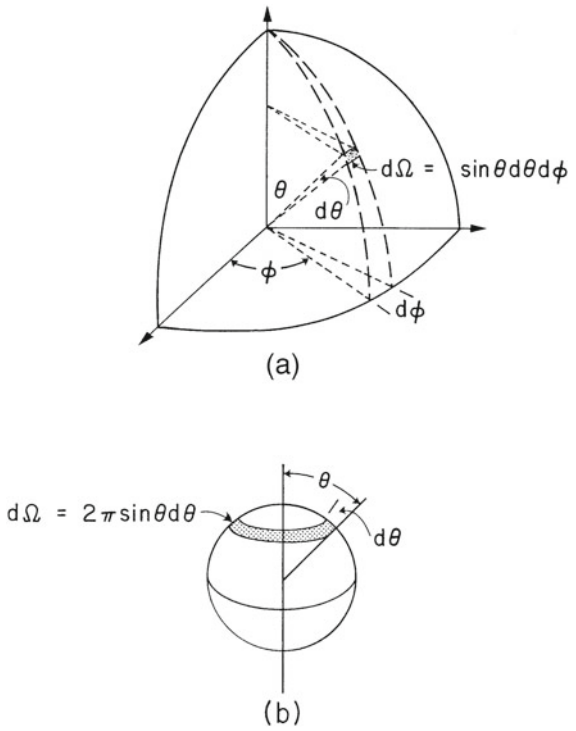

Fig. 14.11 **a** A small solid angle $d\Omega = \sin\theta\, d\theta\, d\phi$ surrounds the direction defined by angles θ and ϕ. **b** The solid angle $d\Omega = 2\pi \sin\theta\, d\theta$ results from integrating over ϕ

the incident particle moves along the z axis, the solid angle is $d\Omega = \sin\theta\, d\theta\, d\phi$ (Appendix L). If the cross section has no ϕ dependence, then the integration over ϕ can be carried out and $d\Omega = 2\pi \sin\theta\, d\theta$. These solid angles are shown in Fig. 14.11.

There are three ways to interpret the exponential decay of the primary beam. First, the number of particles remaining in the beam that have undergone no interaction decreases as the target becomes thicker, so that the number of particles available to interact in the deeper layers is less. Second, the exponential can be regarded as taking into account the fact that in a thicker sample some of the target atoms are hidden behind others and are therefore less effective in causing new interactions. The third interpretation is in terms of the Poisson probability distribution (Appendix J). Each layer of thickness dz provides a separate chance for the beam particles to interact. The probability of interacting in any one layer dz is small, $p = \sigma_{\text{tot}} N_A \rho\, dz/A$, while the total number of "tries" is z/dz. The average number of interactions is $m = p \times$ number of tries. The probability of no interaction is $e^{-m} = \exp(-\sigma_{\text{tot}} N_A \rho\, z/A) = e^{-\mu z}$.

When the cross section for scattering is large, things can become quite complicated. For example, photons may scatter many times and be traveling through the material in all directions. Various approximations have been used to model photon transport in such a case. We will examine some of them shortly. One simple correction that is often made is to consider the average direction a scattered photon travels, for example, the average value of the cosine of the scattering angle, $g = \overline{\cos\theta}$, where θ is the angle of a single scattering. If the average angle of scattering is very small, g is nearly 1. If the photon is scattered backward, $g = -1$, and if the scattering is isotropic, $g = 0$. Formally,

$$g = \frac{\int_0^\pi \sigma(\theta) \cos\theta\, 2\pi \sin\theta\, d\theta}{\int_0^\pi \sigma(\theta)\, 2\pi \sin\theta\, d\theta}. \tag{14.24}$$

The *reduced scattering coefficient*

$$\mu_s' = (1 - g)\mu_s \tag{14.25}$$

is what is usually measured.

The values of the scattering and absorption coefficients vary widely. For infrared light at 780 nm, values are roughly[3]

$$\mu_s' = 1500\,\text{m}^{-1}, \qquad \mu_a = 5\,\text{m}^{-1}.$$

14.6 The Diffusion Approximation to Photon Transport

When photons enter a substance, they may scatter many times before being absorbed or emerging from the substance. This leads to *turbidity*, which we see, for example, in milk or clouds. The most accurate studies of multiple scattering are done with *Monte Carlo* computer simulations, in which probabilistic calculations are used to follow a large number of photons as they repeatedly interact in the tissue being simulated. However, Monte-Carlo techniques use lots of computer time. Various approximate analytic solutions also exist. The field is reviewed in Chap. 5 of Grossweiner (1994).

14.6.1 Diffusion Approximation

One of the approximations, the diffusion approximation, is described here. It is useful when many scattering events occur for each photon absorption. This is a valid approximation for most tissue, but not for cerebrospinal fluid or synovial (joint) fluid.

[3] These are eyeballed from data for various tissues reported in the article by Yodh and Chance (1995). Values are up to ten times larger at other wavelengths. See Table 5.2 in Grossweiner (1994). Nickell et al. (2000) report values for skin that depend on both the direction of propagation and the degree of stretching of the skin. They are similar to the values reported here.

If the photons have undergone enough scattering in a medium, all memory of their original direction is lost. In that case, the movement of the photons can be modeled by the diffusion equation. In Chap. 4, we wrote Fick's second law as

$$\frac{\partial C}{\partial t} = D\nabla^2 C + Q.$$

The left-hand side of the equation is the rate at which the concentration, the number of particles per unit volume, is increasing. The term $D\nabla^2 C$ is the net diffusive flow into the small volume, the particle current being given by $\mathbf{j} = -D\nabla C$. The last term is the rate of production or loss of particles within the volume by other processes, depending on whether Q is positive or negative.

Let us suppose that we can apply this to photons. We will consider two contributions to Q. The concentration must be the number of *diffusing* photons per unit volume. Many in the incident beam are still traveling in the original direction and are not diffusing, but if they are scattered they become part of the diffusing photon pool. Therefore there may be a source term, which we will call s, due to the incident photons. But photons are also being absorbed. They are traveling with a speed $c_n = c/n$, where n is the index of refraction of the medium. In time dt, they travel a distance $dx = c_n dt$, and the probability that they are absorbed is $\mu_a dx = \mu_a c_n dt$. Therefore the diffusion equation for photons is

$$\frac{\partial C}{\partial t} = D\nabla^2 C - \mu_a c_n C + s. \tag{14.26}$$

Each term has the units of photons $\mathrm{m}^{-3}\ \mathrm{s}^{-1}$.

In photon transfer, it is customary to make two changes in this equation. The first is to divide all terms by the speed of the photons in the medium,[4] c_n. The result is

$$\frac{1}{c_n}\frac{\partial C}{\partial t} = D'\nabla^2 C - \mu_a C + \frac{s}{c_n},$$

where $D' = D/c_n$ is referred to in the photon transfer literature as the *photon diffusion constant*. It has dimensions of length.

Two important quantities in radiation transfer are the *photon* or *particle fluence* and the *photon fluence rate*. The International Commission on Radiation Units and Measurements (ICRU) defines the particle fluence for any kind of particle, including photons as follows: At the point of interest construct a small sphere of radius a. Let the number of particles striking the surface of the sphere during some time interval have an *expectation value* N. (The expectation value is the mean of a set of measurements in the limit as the number of measurements becomes infinite.) The particle fluence Φ is the ratio $N/\pi a^2$, where πa^2 is the area of a great circle of the sphere, that is, the area of a circle having the same radius as the sphere. This is shown in Fig. 14.12 and is a generalization of our earlier use of Φ as the number of particles per unit area. It neatly avoids having to introduce obliquity factors, since for any direction the particles travel, one can construct a great circle on the sphere that is perpendicular to their path. The *particle fluence rate* is

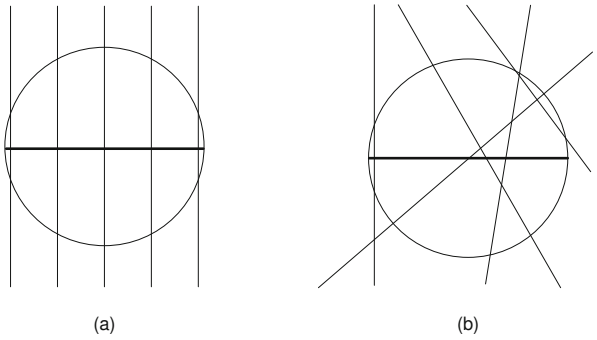

Fig. 14.12 The particle fluence is the ratio of the expectation or average value of the number of particles passing through the sphere to the area of a great circle of the sphere, πa^2. It depends on the total number of particles passing through the sphere, regardless of the direction they travel. The fluence is the same in each case shown: five particles traverse each sphere

$$\varphi = \frac{d\Phi}{dt}.$$

We saw in Chap. 4 that for a group of particles all traveling with the same speed, the number transported across a plane per unit area per unit time is equal to their concentration times their speed. The photon concentration is related to the photon fluence rate by $C = \varphi/c_n$, and the photon diffusion equation becomes

$$\frac{1}{c_n}\frac{\partial \varphi}{\partial t} = D'\nabla^2\varphi - \mu_a\varphi + s. \tag{14.27}$$

This is the form that is usually found in the literature. The units of each term are photons $\mathrm{m}^{-3}\ \mathrm{s}^{-1}$. One can show that[5]

$$D' = \frac{1}{3\left[\mu_a + (1-g)\mu_s\right]} = \frac{1}{3(\mu_a + \mu_s')}. \tag{14.28}$$

14.6.2 Continuous Measurements

If the tissue is continuously irradiated with photons at a constant rate, the term containing the time derivative vanishes. If

[4] Most papers in this field use c as the velocity of light in the medium. We prefer to reserve c for the fundamental constant, the velocity of light in vacuum.

[5] See, for example, Duderstadt and Hamilton (1976, pp. 133–136).

in addition we use a broad beam of photons so that we have a one-dimensional problem and we are far enough into the tissue so that the source term can be ignored, the model is

$$D' \frac{d^2\varphi}{dx^2} = \mu_a \varphi. \tag{14.29}$$

This has an exponential solution $\varphi = \varphi_0 e^{-\mu_{\text{eff}} x}$, where $\mu_{\text{eff}} = \left\{3\mu_a \left[\mu_a + (1-g)\mu_s\right]\right\}^{1/2}$. It is interesting to see what these numbers mean. Using the "typical" values from Sect. 14.5, the number of photons that have not interacted (are not yet attenuated) falls exponentially with a characteristic length or mean depth

$$\lambda_{\text{unatten}} = \frac{1}{\mu} = \frac{1}{\mu_a + \mu_s'} = \frac{1}{1505} = 0.66 \text{ mm}.$$

For the diffuse beam, the mean depth is about ten times this:

$$\lambda_{\text{diffuse}} = \frac{1}{\mu_{\text{eff}}} = \frac{1}{\sqrt{(3)(5)(1505)}} = 6.7 \text{ mm}.$$

These values are for a wavelength where the tissue is fairly transparent. The diffusion equation can be solved for other geometries that model the light source being used.[6] One problem with these measurements is that they give only μ_{eff}, which is a combination of μ_a and μ_s. Also, the path length may be ambiguous because the geometry cannot be modeled accurately.

14.6.3 Pulsed Measurements

A technique made possible by ultrashort light pulses from a laser is *time-dependent diffusion.* It allows determination of both μ_s and μ_a. A very short (150 ps) pulse of light strikes a small region on the surface of the tissue. A detector placed on the surface about 4 cm away records the multiply-scattered photons. A typical plot of the detected photon fluence rate is shown in Fig. 14.13. Patterson et al. (1989) have shown that the reflected fluence rate after a pulse is approximately

$$R(r,t) = \frac{z_0}{(4\pi D' c_n t)^{3/2} t} e^{-\mu_a c_n t} e^{-(r^2+z_0^2)/4D'c_n t}. \tag{14.30}$$

Here r is the distance of the detector from the source along the surface of the skin, $c_n t$ is the total distance the photon has traveled before detection, and $z_0 = 1/\left[(1-g)\mu_s\right]$ is the depth at which all the incident photons are assumed to scatter and become part of the diffuse photon pool. This curve fits Fig. 14.13 well and can be used to determine μ_a and $(1-g)\mu_s$. We can understand the various factors in Eq. 14.30. The last factor is a Gaussian spreading in the

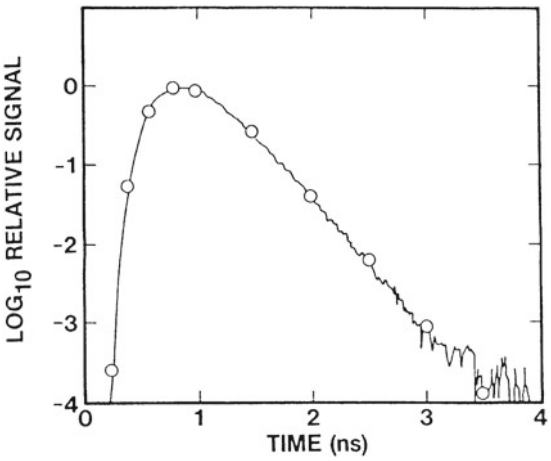

Fig. 14.13 Time-resolved infrared spectroscopy. The line is a measurement of the reflected photons from the calf of a human volunteer at a distance of 4 cm from the pulsed source. The wavelength is 760 nm. The circles are calculated using Eq. 14.30 and normalized to the peak value. (Source: Patterson et al. 1989. Copyright by the Optical Society of America.)

r direction away from the z axis where the photons were injected. This is a two-dimensional problem. Compare this with Eq. 4.77, which shows that in two dimensions $\sigma_r^2 = 4Dt$, and recall that $D = D'c_n$. The middle factor is the fraction of the photons in the pulse that have not been absorbed, $\exp(-\mu_a x)$, where x is the total distance the photons have traveled. The first factor is the normalization that reduces the amplitude of the Gaussian as it spreads.

A related technique is to apply a continuous laser beam whose amplitude is modulated at various frequencies between 50 and 800 MHz. The Fourier transform of Eq. 14.30 gives the change in amplitude and phase of the detected signal. Their variation with frequency can also be used to determine μ_a and μ_s.[7]

14.6.4 Refinements to the Model

The diffusion equation, Eq. 14.27, is an approximation, and the solution given, Eq. 14.30, requires some unrealistic assumptions about the boundary conditions at the surface of the medium ($z = 0$). Hielscher et al. (1995) compared experiment, Monte Carlo calculations, and solutions to the diffusion equation with three different boundary conditions. They found that Eq. 14.30 was the easiest to use but leads to errors in the estimates of the coefficients that become worse when the detector and source are close together. Their Monte Carlo calculations fit the data quite well. They also discuss

[6] See, for example, Grossweiner (1994, p. 98).

[7] See, for example, Sevick et al. (1991) or Pogue and Patterson (1994).

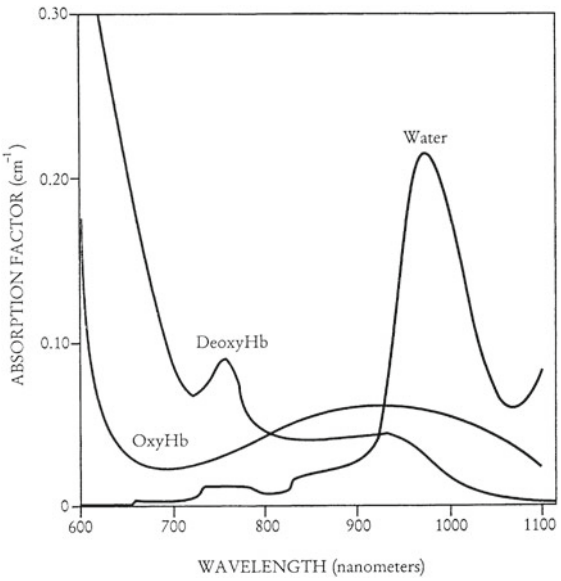

Fig. 14.14 The absorption coefficient μ_a for water, oxyhemoglobin, and deoxyhemoglobin. (Reprinted with permission from Yodh and Chance (1995). Copyright 1995, American Institute of Physics)

the reflections that occur when light goes from one medium into another with a different index of refraction.

14.7 Biological Applications of Infrared Scattering

There are a number of uses of light in the near infrared: some clinical and some in the laboratory.

14.7.1 Near Infrared (NIR)

Near-infrared light in the range 600–1000 nm is used to measure the oxygenation of the blood as a function of time by determining the absorption at two different wavelengths. Figure 14.14 shows the absorption coefficients for oxygenated and deoxygenated hemoglobin and water. The greater absorption of blue light in oxygenated hemoglobin makes oxygenated blood red. (The graph shows only wavelengths longer than 600 nm—red and infrared.) The wavelength 800 nm at which both forms of hemoglobin have the same absorption is called the *isosbestic point*. Measurements of oxygenation are made by comparing the absorption at two wavelengths on either side of this point.

One of the difficulties with these measurements is knowing the path length, since photons undergo many scatterings before being absorbed or reaching the detector. Scattering from many tissues besides hemoglobin distorts the signal. Nonetheless, *pulse oximeters* that fit over a finger are widely used. Webster (1997) provides a comprehensive discussion of the underlying physics, design, calibration, and use of pulse oximeters. The basic feature is that arterial blood flow is pulsatile, not continuous. Therefore, measuring the time-varying (AC) signal selectively monitors arterial blood and eliminates the contribution from venous blood and tissue. Scattering corrections must still be made (Farmer 1997; Wieben 1997).

Development of new applications for infrared scattering measurements continues as new detectors with different spectral sensitivities become available (Yamashita et al. 2001). Continuous sources are also used to determine blood oxygenation of tissue (Liu et al. 1995).

14.7.2 Optical Coherence Tomography (OCT)

Optical range measurements using the time delay of reflected or backscattered light from pulses of a few femtosecond (10^{-15} s) duration can be used to produce images similar to those of ultrasound A- and B-mode scans. The spatial extent of a 30 fs pulse in water is about 7 μm. Since it is difficult to measure time intervals that short, most measurements are done using interference properties of the light. *Optical coherence tomography* is conceptually similar to range measurements but uses interference measurements. It was first demonstrated by Huang et al. (1991) and has been developed extensively since then (see Schmitt 1999; Brezinski 2006 or Fercher et al. 2003). It is widely used in ophthalmology.

This is one topic for which we must use the electromagnetic wave model for light, since it depends on interference effects. Light waves differ from sound waves because the electric field in the wave is a vector perpendicular to the direction of propagation of the wave. This gives rise to an important effect—polarization—that we ignore.

Suppose that a wave $A\sin\frac{2\pi}{\lambda}(x-c_nt) = A\sin\omega(x/c_n - t)$ travels in a medium with index of refraction n. A detector responds to the energy fluence in the wave, which is proportional to the square of the amplitude averaged over time. The signal is $y \propto A^2\overline{\sin^2\omega(x/c_n - t)} = A^2/2$. The wave is split, travels two paths of different lengths, and is recombined at a detector. The signal is proportional to the power averaged over many cycles of the wave. The power is proportional to the square of the electric field:

$$y \propto (A/2)^2\overline{\left[\sin\omega(x_1/c_n - t) + \sin\omega(x_2/c_n - t)\right]^2}$$
$$= \frac{A^2}{4}\left(1 + \cos\frac{\omega}{c_n}(x_2 - x_1)\right). \qquad (14.31)$$

The signal oscillates between 0 and $A^2/2$ as the difference in path length is changed. When the path difference is zero,

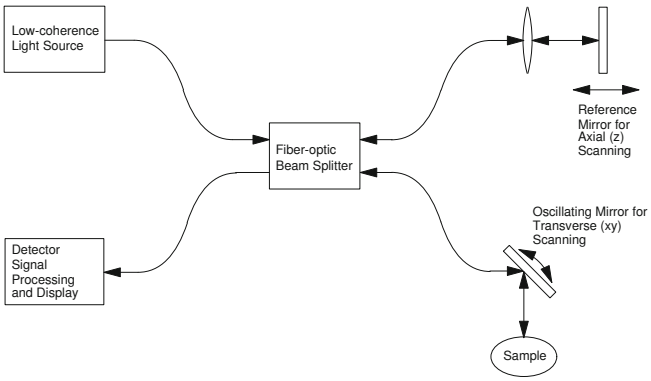

Fig. 14.15 The basic apparatus for optical coherence tomography. The features are described in the text

$y \propto A^2/2$, our original result. This dependence of the signal on path length forms the basis for *interferometry*, which can be used to measure changes in distance with high accuracy—counting maxima (fringes) as one path length is varied.

An important consideration is the *coherence* of the light beam: the number of cycles over which the phase of the wave does not change. When an atom emits light, the classical electromagnetic wave lasts for a finite time, τ_{coh} (often around 10^{-8} s). When another atom emits light, the phase is unrelated to the phase of light already emitted. This means that if $(x_2 - x_1)/c_n > \tau_{\text{coh}}$, the time average will go to zero.

Note that as long as light from a single source has been split and then recombined, the paths can be quite long. The interference fringes will be seen when the light is recombined and the path difference satisfies

$$x_2 - x_1 < c_n \tau_{\text{coh}}. \tag{14.32}$$

This provides a technique for determining the distance of a reflecting object from the light source, forming the basis for optical coherence tomography. A light source with a *short* coherence time is used for high resolution. The basic apparatus is shown in Fig. 14.15. Various light sources are used. The light pulse travels over an optical fiber to a 50/50 beam splitter. Part travels to the sample, where it is reflected back to the 50/50 coupler and then to the detector. The other half of the light goes to the reference mirror, where it is also reflected back to the detector. Changing the position of the reference mirror changes the depth of the image plane in the sample. The lateral beam position is changed to scan the sample, as in an ultrasound B-mode scan. Fig. 14.16 shows an image of the retina.

It is possible to make many kinds of images. Fig. 14.17 shows the parabolic velocity profile of blood flowing in a retinal blood vessel 176 μm diameter. It was obtained by measuring the Doppler shift in light scattered from moving blood cells. It is also possible to image glucose concentration, because glucose modifies the index of refraction and thereby the scattering coefficient (Esenaliev et al. 2001). Images are made of the surface layers of the skin, the eye, the walls of the mouth, teeth, larynx, esophagus, stomach, and intestine.

A number of tissues exhibit *birefringence*—the speed of light in the skin depends on the orientation of the electric field vector of the light wave with the cells in the tissue (de Boer et al. 2002). It is possible to make images with different orientations of the electric field vector to improve the resolution (Yasuno et al. 2002).

There are a number of offshoots to OCT, such as optical coherence microscopy and full-field OCM (Saint-Jalmes et al. 2002).

14.7.3 Raman Spectroscopy

Infrared and microwave probes are used extensively in the laboratory. Since the vibrational and rotational levels depend on the masses, separations, and forces between the various atoms bound in a molecule, it is not surprising that spectroscopy can be used to identify specific bonds. This is a useful technique in chemistry. Biological applications are difficult because the absorption coefficients are large; thin samples must be used, particularly in an aqueous environment.

One way around this is *Raman scattering*: the scattering of light in which the scattered photon does not have its original energy, but has lost or gained energy corresponding to a rotational or vibrational transition. The effect was discovered by C. V. Raman in 1928. Raman scattering can be done with light of any wavelength, from infrared to ultraviolet. An idealized example is shown in Fig. 14.18. If the scattering molecule was originally in the vibrational ground state and returns to a vibrational excited state, the Raman-scattered photon has less energy than the original photon. This is called *Stokes-Raman* scattering. If the scattering molecule was originally in a higher vibrational state and returns to the vibrational ground state, the Raman-scattered photon has higher energy than the original. The intensity of this *Anti-Stokes Raman* line will be less than the intensity of the Stokes-Raman line because populations of the original vibrational levels are governed by a Boltzmann factor. Figure 14.19 shows the Stokes-Raman shift spectrum for cholesterol. Many discussions of Raman spectroscopy are available. A fairly theoretical one by Berne and Pecora (1976) relies heavily on autocorrelation functions and spectral analysis that we saw in Chap. 11. Diem (1993) is a detailed text on vibrational spectroscopy, including Raman spectroscopy.

Raman spectroscopy has been used extensively for laboratory studies; many groups are exploring its utility for in vivo

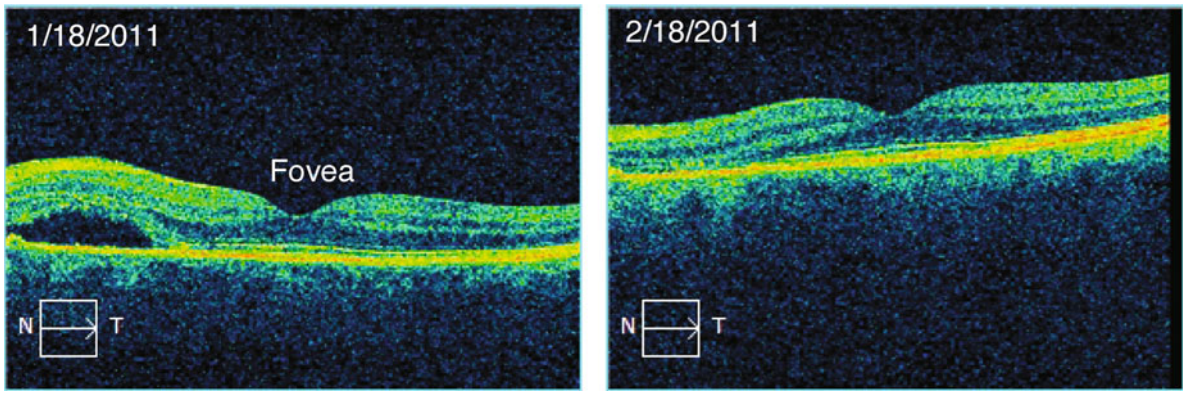

Fig. 14.16 Optical coherence tomograms of the retina. The square box in the lower left corner is about 500 μm on a side. *N* and *T* indicate nasal and temporal. The patient has a subchoroidal neovascular membrane (a collection of new and fragile blood vessels that leak) seen as a pocket of fluid on the left. The lesion was treated with a laser (photocoagulation). The tomogram 1 month later shows resolution of the fluid pocket. (Scans courtesy of Kirk Morgan, MD)

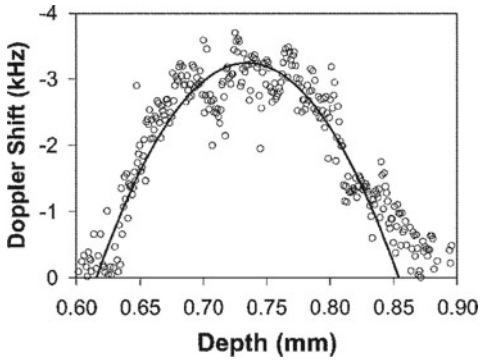

Fig. 14.17 The parabolic velocity profile of blood flowing in a single retinal vessel of diameter 176 μm. (Source: Yazdanfar et al. 2000. Used by permission)

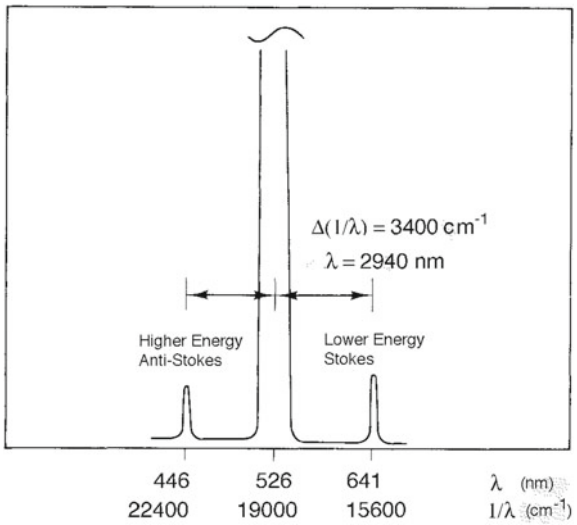

Fig. 14.18 In Raman scattering, a photon gains or loses energy due to a change in the energy of the scattering molecule. An idealized example for water is shown. The very intense line (the tall peak) has no energy change; the weak lines are Raman scattering. The abscissa is shown as wavelength λ and as reduced wave number $k/2\pi = 1/\lambda$. The Raman shift corresponds to $\Delta(1/\lambda) = 3400\ \text{cm}^{-1}$. The wavelength of this infrared transition is $\lambda = 2940$ nm, but the measurement is made near 500 nm

measurements (Hanlon et al. 2000). Infrared light between 800 and 1000 nm is usually used.

14.7.4 Far Infrared or Terahertz Radiation

For many years, there were no good sources or sensitive detectors for radiation between microwaves and the near infrared (0.1–100 THz). Developments in optoelectronics have solved both problems, and many investigators are exploring possible medical uses of THz radiation ("T rays"). Classical electromagnetic wave theory is needed to describe the interactions, and polarization (the orientation of the **E** vector of the propagating wave) is often important. The high attenuation of water in this frequency range means that studies are restricted to the skin or surface of organs such as the esophagus that can be examined endoscopically. Reviews are provided by Smye et al. (2001), Fitzgerald et al. (2002), and Zhang (2002). See the article by Armstrong (2012) for a survey of the challenges of using terahertz radiation.

14.8 Thermal Radiation

Any atomic gas emits light if it is heated to a few thousand kelvin. The light consists of a line spectrum. The famous yellow line of sodium has

$$\lambda = 589.2\ \text{nm},$$

$$\nu = c/\lambda = 509.2\ \text{THz},$$

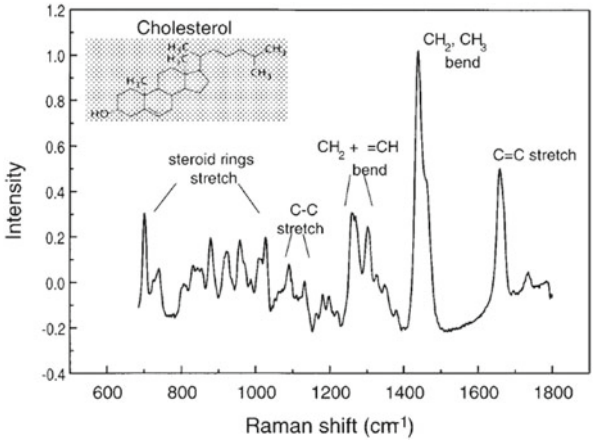

Fig. 14.19 Vibrational Raman lines for cholesterol. A continuous background has been subtracted. The abscissa is $1/\lambda = E/hc$. (Source: Hanlon et al. 2000. Used by permission)

Table 14.3 Approximate color temperatures. The range of values reflects differences between scales established by different observers

Color	T (K)
Red, just visible in daylight	750–800
"Cherry" red	975–1175
Yellow	3000–4000
White	5000–6000
Dazzling (bluish white)	> 10 000

$$E = h\nu = hc/\lambda = 3.38 \times 10^{-19}\ \text{J} = 2.11\ \text{eV}.$$

These photons are emitted when sodium atoms lose 2.11 eV and return to their ground state. If the sodium atoms are excited by thermal collisions, the probability that a sodium atom is in the excited state, relative to the probability that it is in the ground state, is given by the Boltzmann factor

$$\frac{P_{\text{excited}}}{P_{\text{ground}}} = e^{-E/k_B T}.$$

At room temperature $k_B T = 4.14 \times 10^{-21}$J, so $e^{-E/k_B T} = e^{-81.5} = 3.8 \times 10^{-36}$. The number of atoms in the excited state is utterly negligible. If the temperature is raised to 1500 K, $e^{-E/k_B T}$ is 8×10^{-8}, and enough atoms are excited to give off light as they fall back to the ground state.

If a piece of iron is heated to 1500 K, it glows with a red–orange color. Table 14.3 relates apparent color to temperature for a glowing metal. If the light is analyzed with a spectroscope, it is found to consist of a continuous range of colors rather than discrete lines.

The difference between the spectra of single atoms and the spectra of solids and liquids can be understood from the following argument. If we have N isolated identical atoms, each atom has an energy level at the energy shown in Fig. 14.20a. There are a total of N levels, one for each atom. When two of these atoms are brought close together,

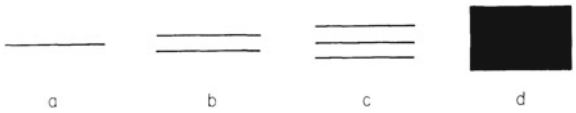

Fig. 14.20 The splitting of energy levels as many atoms are brought together. **a** A single atom. **b** Two atoms. **c** Three atoms. **d** Many atoms

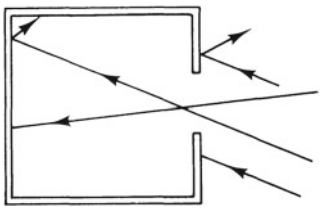

Fig. 14.21 A small hole in the wall of a cavity is a better blackbody than the walls of the cavity are. Any light that enters the hole must be reflected several times before emerging. It can be absorbed by the wall at any reflection. If the walls appear black, the hole appears even blacker. (The walls are highly absorbing diffuse reflectors)

the levels shift slightly and split into two closely spaced levels because of interaction between the atoms. The two levels for a pair of atoms are shown in Fig. 14.20b. If three atoms are brought close together, the level splits into three levels as shown in Fig. 14.20c. If a large number of atoms are brought close together, the N levels spread out into a *band*, Fig. 14.20d. Transitions from one band to another can have many different energies, and photons with a continuous range of energies can be emitted or absorbed.

The relative number of photons of different energies that will be emitted or absorbed depends on the nature of the substance. Glass and sodium chloride crystals are nearly transparent in the visible spectrum because the spacing of the levels is such that no photons of these energies are absorbed. When such substances are heated enough to populate the higher energy levels, no photons of these energies are emitted.

A substance that has so many closely spaced levels that it can absorb every photon that strikes it appears black. It is called a *blackbody*. It is difficult if not impossible to make a surface that is completely absorbing; the absorption can be improved by making a cavity, as in Fig. 14.21. Photons entering the hole in the cavity bounce from the walls many times before chancing to pass out through the hole again, and they therefore have a greater chance of being absorbed. Such a hole in a cavity is a better approximation to a blackbody than is the absorbing material lining the cavity.

If the surface is not completely absorbing, we define the *emissivity* $\epsilon(\lambda)$, which is the fraction of light absorbed at wavelength λ. (Why emission and absorption are closely related is discussed below.) If the light all passes through some transparent material or is completely reflected, then $\epsilon = 0$; if

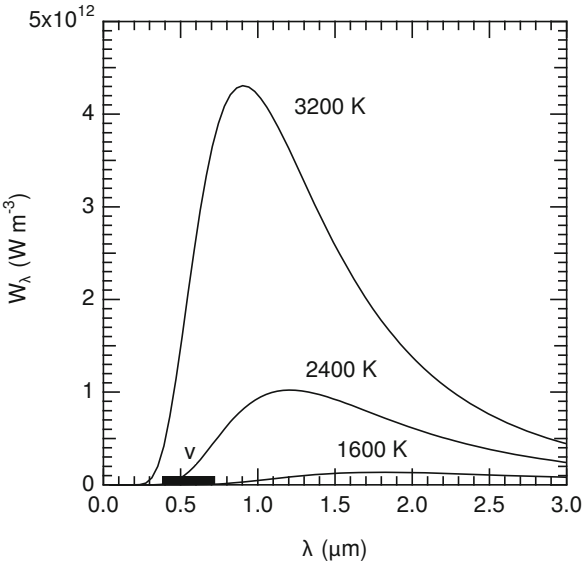

Fig. 14.22 The blackbody radiation function for several temperatures. The visible spectrum is marked by v

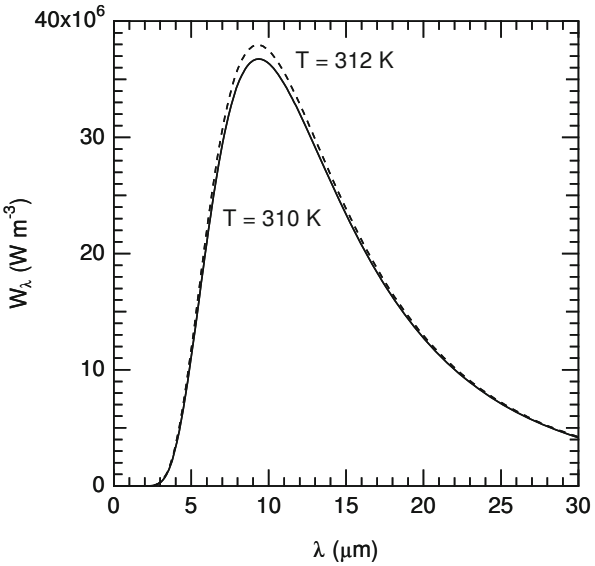

Fig. 14.23 The blackbody radiation function $W_\lambda(\lambda, T)$ for $T = 310$ K and $T = 312$ K

it is all absorbed, $\epsilon = 1$. A blackbody has $\epsilon(\lambda) = 1$ for all wavelengths. An object for which $\epsilon(\lambda)$ is constant but less than 1 is called a gray body.

When a blackbody is heated, the light given off has a continuous spectrum because the energy levels are so closely spaced. By imagining two interacting black bodies in equilibrium, one can argue[8] that the amount of energy emitted by a blackbody depends only on its temperature and not on the nature of the surfaces.

The spectrum of power per unit area emitted by a completely black surface in the wavelength interval between λ and $\lambda + d\lambda$ is

$$W_\lambda(\lambda, T)d\lambda,$$

a universal function called the *blackbody radiation function*. It has units of W m^{-3}, although it is often expressed as W cm^{-2} μm^{-1}. The value of W_λ is plotted for several different temperatures in Fig. 14.22. As the black surface or cavity walls become hotter, the spectrum shifts toward shorter wavelengths, which is consistent with the observations in Table 14.3. The visible region of the spectrum is marked on the abscissa in Fig. 14.22; even at 3200 K, most of the energy is radiated in the infrared.

Figure 14.23 plots $W_\lambda(\lambda, T)$ for two temperatures near body temperature (37° C=310 K). Compare the scales of Figs. 14.22 and 14.23, and note how much more energy is emitted by a blackbody at the higher temperature and how it is shifted to shorter wavelengths.

Much work was done on the properties of blackbody or thermal or cavity radiation in the late 1800s and early 1900s. While some properties could be explained by classical physics, others could not. The description of the function $W_\lambda(\lambda, T)$ by Max Planck is one of the foundations of quantum mechanics. We will not discuss the history of these developments, but will simply summarize the properties of the blackbody radiation function that are important to us.

The value of $W_\lambda(\lambda, T)$ is given by

$$W_\lambda(\lambda, T) = \frac{2\pi c^2 h}{\lambda^5 \left(e^{hc/\lambda k_B T} - 1\right)}. \tag{14.33}$$

Consider the expression $e^{hc/\lambda k_B T}$ in the denominator. Since light consists of photons of energy $E = h\nu = hc/\lambda$, the expression in parentheses in the denominator is $e^{E/k_B T} - 1$. For very large energies (short wavelengths) the 1 can be neglected and this expression is the Boltzmann factor.

We can find the total amount of power emitted per unit surface area by integrating[9] Eq. 14.33:

$$\begin{aligned} W_{\text{tot}}(T) &= \int_0^\infty W_\lambda(\lambda, T)d\lambda \\ &= \frac{2\pi^5 k_B^4}{15c^2h^3} T^4 = \sigma_{SB} T^4. \end{aligned} \tag{14.34}$$

This is the *Stefan–Boltzmann law*. The Stefan–Boltzmann constant, which is traditionally denoted by σ_{SB} but which

[8] For a brief discussion, see Schroeder (2000).

[9] This is not a simple integration. See Gasiorowicz (2003, p. 3).

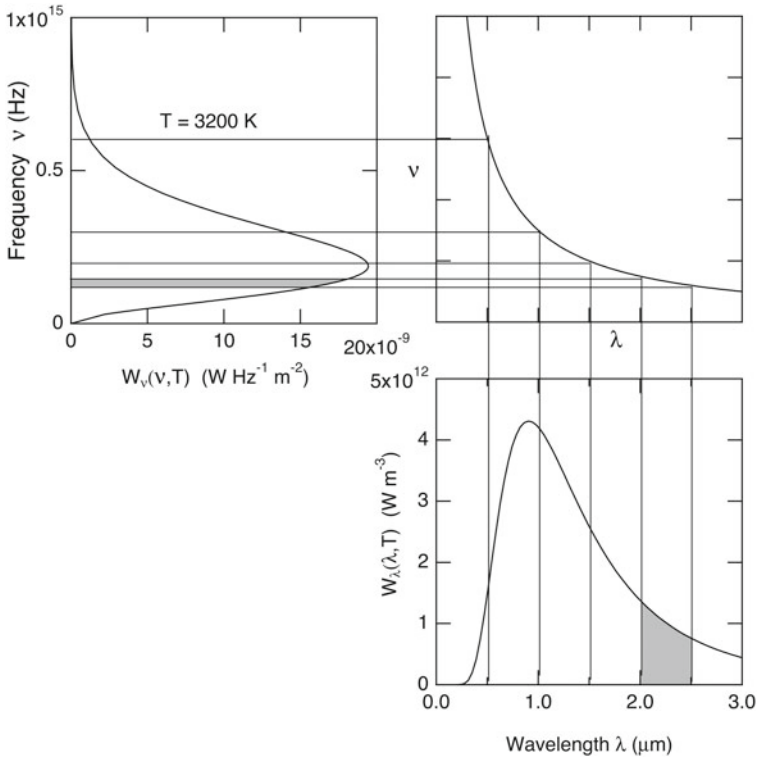

Fig. 14.24 The transformation from $W_\lambda(\lambda, T)$ to $W_\nu(\nu, T)$ is such that the same amount of power per unit area is emitted in wavelength interval $(\lambda, d\lambda)$ and the corresponding frequency interval $(\nu, d\nu)$. (For example, the two shaded areas are the same.) The spectrum shown is for a blackbody at 3200 K

has no relationship to cross section, was known empirically before Planck's work. It has the numerical value

$$\sigma_{SB} = 5.67 \times 10^{-8} \text{W m}^{-2} \text{ K}^{-4}. \tag{14.35}$$

Early experiments were performed with equipment that measured the radiation function versus wavelength. It is also possible to measure versus frequency. To rewrite the radiation function in terms of frequency, let λ_1 and $\lambda_2 = \lambda_1 + d\lambda$ be two slightly different wavelengths, with power $W_\lambda(\lambda, T)d\lambda$ emitted per unit surface area at wavelengths between λ_1 and λ_2. The same power must be emitted[10] between frequencies $\nu_1 = c/\lambda_1$ and $\nu_2 = c/\lambda_2$:

$$W_\nu(\nu, T)d\nu = W_\lambda(\lambda, T)d\lambda. \tag{14.36}$$

Since $\nu = c/\lambda$, $d\nu/d\lambda = -c/\lambda^2$, and

$$|d\nu| = +\frac{c}{\lambda^2}\,|d\lambda|\,. \tag{14.37}$$

[10] $W_\lambda(\lambda, T)$ and $W_\nu(\nu, T)$ do not have the same functional form. In fact, they have different units. The units of $W_\lambda(\lambda, T)$ are W m^{-3}, while those of $W_\nu(\nu, T)$ are W s m^{-2}.

Equations 14.33–14.37 can be combined to give

$$W_\nu(\nu, T) = \frac{2\pi\nu^2(h\nu)}{c^2(e^{h\nu/k_BT} - 1)}. \tag{14.38}$$

This transformation is shown in Fig. 14.24. The amount of power per unit area radiated in the 0.5-μminterval between two of the vertical lines in the graph on the lower right is the area under the curve of W_λ between these lines. The graph on the upper right transforms to the corresponding frequency interval. The radiated power, which is the area under the W_ν curve between the corresponding frequency lines on the upper left, is the same. Note that the peaks of the two curves are at different frequencies or wavelengths. We will see this same transformation again when we deal with x rays. We see in the figures above that at higher temperatures the peak occurs at shorter wavelengths. Equation 14.33 can be differentiated to show that at temperature T, the peak in W_λ occurs at wavelength

$$\lambda_{\max} T = \frac{hc}{4.9651 k_B} = 2.90 \times 10^{-3} \text{ m K}. \tag{14.39}$$

Similarly, we can differentiate Eq. 14.38 to show that

$$\frac{\nu_{\max}}{T} = \frac{2.82144 k_B}{h} = 5.88 \times 10^{10} \text{ K}^{-1}\text{s}^{-1}.$$

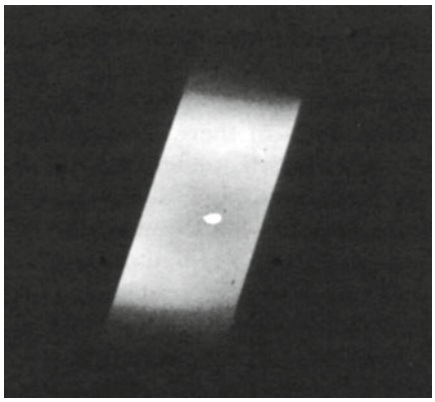

Fig. 14.25 A photograph of an incandescent tungsten tube with a small hole drilled in it. The radiation emerging from the hole is brighter than that from the tungsten surface. (Source: Halliday et al. (1992). Copyright ©1992 John Wiley & Sons. Reproduced by permission of John Wiley & Sons)

The product $\lambda_{\max}\nu_{\max} = 1.705 \times 10^8 \text{m s}^{-1} = 0.57c$.

All this is true for a blackbody. Thermodynamic arguments can be made to show that if a body does not completely absorb light at some wavelength, that is $\epsilon(\lambda) < 1$, then the power emitted at that wavelength is

$$\epsilon(\lambda) W_\lambda(\lambda, T). \tag{14.40}$$

This is the same $\epsilon(\lambda)$ that was introduced earlier in this section. It is called the *emissivity* of the surface. This implies that a surface that appears blackest when it is absorbing radiation will be brightest when it is heated. Figure 14.25 shows a small hole in a piece of tungsten that has been heated. The hole forms the opening to a cavity and is therefore more absorbing than is the tungsten surface. When heated, the hole emits more light than the tungsten surface.

14.9 Infrared Radiation from the Body

The body radiates energy in the infrared, and this is a significant source of energy loss. Infrared radiation has been used for over 40 years to image the body, but the value of the technique is still a matter of debate. We saw earlier how the *scattering* of infrared radiation by the body can be used to learn information about tissue beneath the surface.

Measurements of the emissivity of human skin have shown that for 1 μm $< \lambda \leq$ 14 μm, $\epsilon(\lambda) = 0.98 \pm 0.01$. This value was found for white, black, and burned skin (Steketee 1973). In the infrared region in which the human body radiates, the skin is very nearly a blackbody. Let us apply Eq. 14.34 to see what the blackbody radiation from the human body is. The total surface area of a typical adult male is about 1.73 m^2. The surface temperature is about

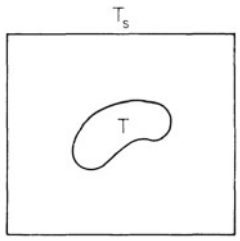

Fig. 14.26 A blackbody at temperature T within a container with wall temperature T_s

33 °C = 306 K (this is less than the core temperature of 310 K). Therefore the total power radiated is $w_{\text{tot}} = SW_{\text{tot}} = S\sigma_{SB}T^4 = 860$ W. This is a large number, nearly nine times the basal metabolic rate of 100 W. The reason it is so large is that it assumes the surroundings are at absolute zero, or that the subject is radiating in empty space with no surroundings. When there are nearby surfaces, radiation from them is received by the subject, and the net radiation is considerably less than 860 W. The easiest arrangement for which to calculate the net heat loss is a blackbody at temperature T surrounded by a similar surface at temperature T_s (Fig. 14.26). At equilibrium the temperature of both objects is the same, $T = T_s$ and the power emitted by the body is equal to the power absorbed. Increasing T increases the power emitted according to $W_{\text{tot}} = \sigma_{SB}T^4$. The body then emits more power than it absorbs. Equilibrium is restored when the body has cooled or the surroundings have warmed so that the temperatures are again the same. Thermodynamic arguments can be made to show that the net power radiated by the body is

$$w_{\text{tot}} = S\sigma_{SB}(T^4 - T_s^4). \tag{14.41}$$

If the object is not a blackbody or the wall temperature is not uniform, the net power loss is more complicated. However, this model represents a considerable improvement over our previous calculation. Suppose that the surroundings are at a temperature $T_s = 293$ K (20 °C). The net loss is

$$w_{\text{tot}} = (1.73)(5.67 \times 10^{-8})(306^4 - 293^4) = 137 \text{ W}.$$

This says that a nude subject surrounded by walls at 20 °C would have to exercise to maintain body temperature, even if the air temperature were warm enough so that heat conduction and convection losses were zero.

If you have lived in a cold climate, you have probably felt cold in a room at night when the drapes are open, even though a thermometer records air temperatures that should be comfortable. This is because of radiation from you to the cold window. The glass is transparent only in the visible range; for infrared radiation it is opaque and has a high emissivity. The

radiation of the cold window back to you is much less than your radiation to it, and you feel cold.

This same problem can occur with a premature infant in an incubator. If the incubator is placed near a window, one wall of the incubator can be cooled by radiation to the window. The infant can be cooled by radiation to the wall of the incubator, even though a shiny (low-emissivity) thermometer in the incubator records a reasonable air temperature. One solution is to be careful where an incubator is placed and insulate its walls; another is to redesign incubators with a feedback loop controlling the infant's temperature.

Infrared radiation can be used to image the body. Two types of infrared imaging are used. In infrared photography the subject is illuminated by an external source with wavelengths from 700 to 900 nm. The difference in absorption between oxygenated and deoxygenated hemoglobin allows one to view veins lying within 2 or 3 mm of the skin. Either infrared film or a solid-state camera can detect the reflected radiation.

Thermal imaging detects thermal radiation from the skin surface. Significant emission from human skin occurs in the range 4–30 μm, with a peak at 9 μm (Fig. 14.23). The detectors typically respond to wavelengths below 6–12 μm. *Thermography* began about 1957 with a report that skin temperature over a breast cancer was slightly elevated. There was great hope that thermography would provide an inexpensive way to screen for breast cancer, but there have been too many technical problems. Normal breasts have more variability in vascular patterns than was first realized, so that differences of temperature at corresponding points in each breast are not an accurate diagnostic criterion. The thermal environment in which the examination is done is extremely important. The sensitivity (ability to detect breast cancer) is too low to use it as a screening device. Thermography has also been proposed to detect and to diagnose various circulatory problems. Thermography is not widely accepted (Blume 1993; Vreugdenburg et al. 2013), though it still has its proponents (Lahiri et al. 2012).

Infrared radiation from the tympanic membrane (eardrum) and ear canal is used to measure body temperature. One instrument is based on a *pyroelectric* crystal, which generates a voltage when heated (Fraden 1991). The sensors have a permanent electric dipole moment whose magnitude changes with temperature.

14.9.1 Atherosclerotic Coronary Heart Disease

Atherosclerotic coronary heart disease (ACHD) has been or is being studied with every imaging technique described in this book. All of the techniques are invasive: a *catheter* is inserted into the artery in question. In ACHD, a fatty *plaque* forms in the *lumen* (interior passageway) of the artery.

The standard technique is coronary artery *angiography:* the heart is imaged by x-ray fluoroscopy (see Chap. 16) while a dye opaque to x rays is introduced in the vessel. This allows accurate determination of the degree of *stenosis* (blocking) of the vessel. It has been thought that when the artery is nearly blocked, the restricted blood flow leads to a *myocardial infarct* (heart attack). It has recently been realized that smaller plaques may become disrupted and lead to a myocardial infarct. Current research seeks to learn what makes these particular plaques *vulnerable*. There is an extensive literature, reviewed by MacNeill et al. (2003) and Verheye et al. (2002).

In *intravascular ultrasound* (IVUS), a 20–40 MHz transducer at the end of the catheter can detect calcium (which deposits in areas of tissue injury). IVUS *elastography* measures how the arterial wall changes during the pressure variations of the cardiac cycle, in the hope that changes in elasticity will indicate vulnerable plaques.

Coronary *angioscopy* attempts to directly view the arterial wall using a tiny fiber-optic *endoscope*. A serious problem here is blood getting between the tip of the endoscope and the arterial wall. This has been solved by temporarily *occluding* (blocking) the artery "upstream" with a balloon catheter or by flushing the area with saline solution.

Thermography has also been explored, first with a temperature-sensitive thermistor, and also with an infrared imaging mirror. Areas of inflammation have a somewhat higher temperature than surrounding areas.

Both Raman spectroscopy and near-infrared spectroscopy have been used.

In intravascular magnetic resonance imaging (MRI is described in Chap. 18), the detector coil is made small enough to fit at the tip of the catheter.

14.9.2 Photodynamic Therapy

Photodynamic therapy (PDT) uses a drug called a photosensitizer that is activated by light (Zhu and Finlay 2008; Wilson and Patterson 2008). PDT can treat accessible solid tumors such as basal cell carcinoma, a type of skin cancer (see Sect. 14.10.4). An example of PDT is the surface application of 5-aminolevulinic acid, which is absorbed by the tumor cells and is transformed metabolically into the photosensitizer protoporphyrin IX. When this molecule interacts with light in the 600–800-nm range (red and near infrared), often delivered with a diode laser, it converts molecular oxygen into a highly reactive singlet state that causes necrosis, apoptosis (programmed cell death), or damage to the vasculature that can make the tumor ischemic. Some internal tumors can be treated using light carried by optical fibers introduced through an endoscope.

14.10 Blue and Ultraviolet Radiation

The energy of individual photons of blue and ultraviolet light is high enough to trigger chemical reactions in the body. These can be both harmful and beneficial. A beneficial effect is the use of blue light to treat neonatal jaundice. The most common harmful effect is the development of sunburn, skin cancer, and premature aging of the skin.

14.10.1 Treatment of Neonatal Jaundice

Neonatal jaundice occurs when *bilirubin* builds up in the blood. Bilirubin is a toxic waste product of the decomposition of the hemoglobin that is released when red blood cells die (*hemolysis*). Bilirubin is insoluble in water and cannot be excreted through either the kidney or the gut. It is excreted only after being conjugated with glucuronic acid in the liver. Bilirubin monoglucuronate and bilirubin diglucuronate are both water soluble. They are excreted in the bile and leave via the gut. Some newborns have immature livers that cannot carry out the conjugation. In other cases there is an increased rate of hemolysis, and the liver cannot keep up. The serum bilirubin level can become quite high, leading to a series of neurological symptoms known as *kernicterus*. The abnormal yellow color of the skin called *jaundice* is due to bilirubin in the capillaries under the skin.

When the skin of a newborn with jaundice is exposed to bright light, the jaundice color goes away. Photons of blue light have sufficient energy to convert the bilirubin molecule into more soluble and apparently less harmful forms (McDonagh 1985). Photons of longer wavelength have less energy and are completely ineffective. The standard form of phototherapy used to be to place the baby "under the lights." Since the lights were bright and also emitted some ultraviolet, it was necessary to place patches over the baby's eyes. Also, since the baby's skin had to be exposed to the lights, it had to be placed in an incubator to keep it warm. A fiberoptic blanket has been developed that can be wrapped around the baby's torso under clothing or other blankets. The optical fibers conduct the light from the source directly to the skin. Eye patches are not needed, and the baby can be fed and handled. Typical energy fluence rates are $(4–6) \times 10^{-2}$ W m^{-2} nm^{-1} in the range 425–475 nm. Acceptance by nursing staff and parents is very high (Murphy and Oellrich 1990). The blanket can be used for home treatment.

14.10.2 The Ultraviolet Spectrum

Ultraviolet light can come from the sun or from lamps. The maximum intensity of solar radiation is in the green, at about 500 nm. The sun emits approximately like a thermal radiator at a temperature of 5800 K. Figure 14.27 shows a 5800 K thermal radiation curve. The power per unit area from the sun at all wavelengths striking the earth's outer atmosphere, the *solar constant*, calculated by regarding the sun as a thermal radiator, is 1390 W m^{-2}. Satellite measurements give 1372 W m^{-2} (Madronich 1993). Because of reflection, scattering, atmospheric absorption, and so forth, the amount actually striking the earth's surface is about 1000 W m^{-2}. Figure 14.27 also shows the effect of absorption of sunlight in the atmosphere. The sharp cut off at 320 nm is due to atmospheric ozone (O_3), which absorbs strongly from 200 to 320 nm. Molecular oxygen absorbs strongly below 180 nm.

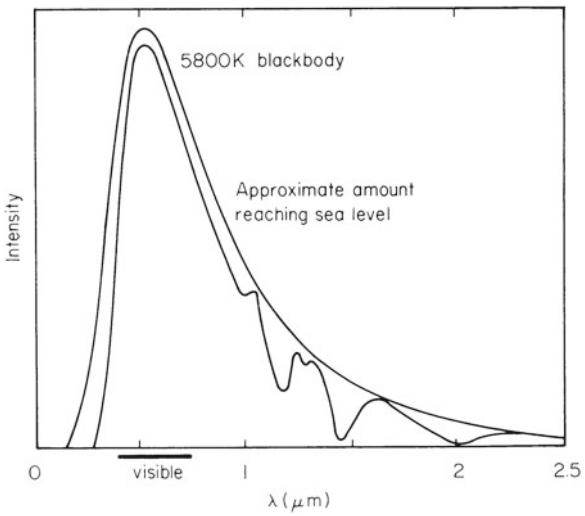

Fig. 14.27 The solar spectrum and the approximate spectrum reaching the earth after atmospheric attenuation

The ultraviolet spectrum is qualitatively divided into the following regions:

UVA	315–400 nm
UVB	280–315 nm[11]
UVC or middle UV	200–280 nm
Far UV	120–200 nm
Extreme UV	10–120 nm

Only the first three are of biological significance, because the others are strongly absorbed in the atmosphere.

Madronich (1993) gives a detailed discussion of the various factors that reduce the ultraviolet energy reaching the earth's surface. The sensitivity of DNA decreases as the wavelength increases. Figure 14.28 shows the solar radiation reaching the ground when the sun is at different angles from the zenith (directly overhead), weighted for DNA sensitivity.

[11] In Europe the range of UVB radiation is 290–300 nm.

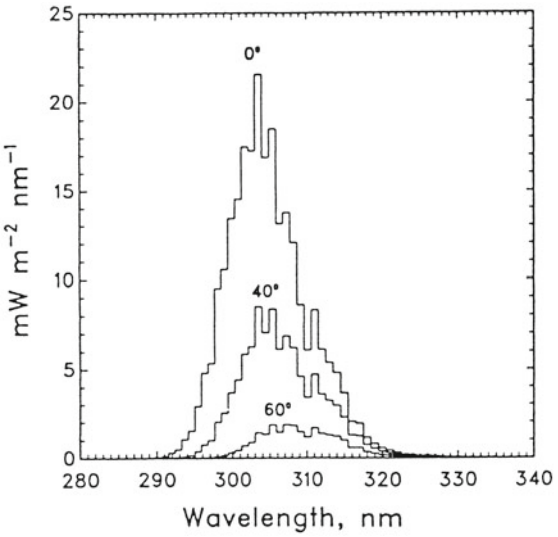

Fig. 14.28 Spectral dose rates weighted for ability to damage DNA for three different angles of the sun from overhead. The calculation assumes clear skies and an ozone layer of 300 Dobson units (1 DU = 2.69×10^{20} molecule m^{-2}). (Source: Madronich (1993). With kind permission of Springer Science and Business Media.)

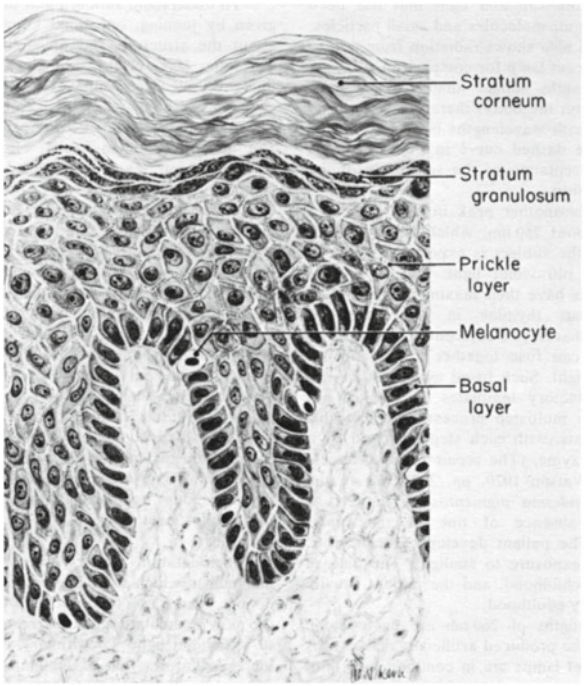

Fig. 14.29 The epidermis. The basal layer contains the cells from which the other layers are derived. As the cells move toward the surface they become the prickle layer and the stratum granulosum. The stratum corneum is dead cellular debris. The melanocytes, which produce melanin granules, are in the basal layer. (Reprinted from Pillsbury and Heaton 1980 with permission from Elsevier.)

Biological effects of ultraviolet light are reviewed by Diffey (1991).

14.10.3 Response of the Skin to Ultraviolet Light

There are several responses of the skin to ultraviolet light. In order to understand them one must know something about the anatomy and physiology of skin. The outer layer of the skin, the *epidermis*, consists of three sublayers (Fig. 14.29). A single layer of *basal cells* is on the inside. Most of these cells produce keratin, a protein that gives the outer layers of skin its strength. About 10 % of the cells are *melanocytes* that produce the pigment *melanin*. Next comes a sublayer of about seven cells, called the *prickle layer*. On top of this is a two- or three-cell layer called the *stratum granulosum* or granular layer. The surface is a layer of dead cells, primarily *keratin* and cellular debris, called the *stratum corneum* or horny layer. Basal cells are constantly produced in the basal layer, migrate outward, become the stratum corneum, and are sloughed off.

In order to discuss injury to tissue, both here by ultraviolet light and in later chapters by x rays, we need to introduce some specialized terms. The body's immediate (*acute*) response to an injury, whether it is an infection, a bump, a cut or a burn, is the *inflammatory response* described on page 122. Prolonged (*chronic*) irritation may result in abnormal cell growth. The abnormalities that result in organs or tissues that are larger than normal are *hypertrophy*, an enlargement of existing cells, and *hyperplasia*, an enlargement due to the formation of new cells. The aberrations in cell growth patterns are shown in Table 14.4. They are *metaplasia*, *dysplasia*, and *anaplasia*. Metaplasia is reversible and goes away if the stimulus or irritant is removed. Dysplasia is sometimes reversible and sometimes progresses to become cancerous. Anaplastic changes are present in nearly all forms of cancer. Anaplasia may result from dysplasia, or it may arise directly from normal cells.

The acute effect of ultraviolet radiation is reddening of the skin or *erythema* due to increased blood flow in the *dermis*, the layer beneath the epidermis. This is part of the inflammatory reaction. The amount of energy that just produces detectable erythema is called the *minimum erythemal dose*. The 1987 *erythema action spectrum* adopted by the CIE[12] shows the relative sensitivity of the skin versus wavelength

[12] *Commission International de l'Eclairage* or International Commission on Illumination.

Table 14.4 Abnormal changes in tissue

Metaplasia	A reversible change in which one cell type is replaced by another.
Dysplasia	Variation in size, shape, and organization of the cells. Literally, "deranged development"
Anaplasia	A marked, irreversible, and regressive change from adult cells that are differentiated in form to more primitive, less differentiated cells

Differences between benign and malignant tumors

Characteristic	Benign	Malignant
Histologic differentiation (microscopic appearance)	Often typical of the tissue of origin	Not well differentiated; atypical cells
Mode of growth	Expands inside a capsule	Expansive; also infiltrative, with no capsule
Rate of growth	Progressive; usually slow; few cells undergoing mitosis (division)	May be rapid, with many cells undergoing mitosis
Metastasis (distant spread)	Absent	Frequently present

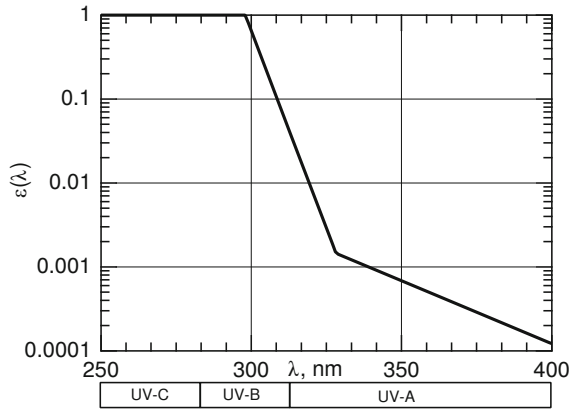

Fig. 14.30 The erythema action spectrum $\epsilon(\lambda)$ for ultraviolet light, as adopted by the CIE in 1987

for the production of erythema. It is

$$\epsilon(\lambda) = \begin{cases} 1.0, & 250 \le \lambda \le 298 \text{ nm} \\ 10^{0.094(298-\lambda)}, & 298 \le \lambda \le 328 \text{ nm} \\ 10^{0.015(139-\lambda)}, & 328 \le \lambda \le 400 \text{ nm}. \end{cases} \quad (14.42)$$

This is plotted in Fig. 14.30. The minimum erythemal dose at 254 nm is about 6×10^7 J m^{-2}. Early effects on skin include sunburn, tanning (now thought to be an injury response), and thickening. Daily exposure for 2–7 weeks causes a three- to fivefold thickening of the stratum corneum.

Some patients have an abnormally high sensitivity to ultraviolet exposure. They may exhibit abnormal photosensitivity because of various diseases or from taking drugs such as phenothiazines (a class of tranquilizers), sulfa drugs, dimethylchlortetracycline, the antidiabetic sulfonureas, thiazide diuretics, and even from drinking quinine water. Photocontact dermatitis is caused by interaction of photons with substances placed on the skin, such as perfumes containing furocoumarins, lime peel, fungi, and fluorescein dye used in lipsticks.

14.10.4 Ultraviolet Light Causes Skin Cancer

Chronic exposure to ultraviolet radiation causes premature aging of the skin. The skin becomes leathery and wrinkled and loses elasticity. The characteristics of photo-aged skin are quite different from skin with normal aging (Kligman 1989). UVA radiation was once thought to be harmless. We now understand that UVA radiation contributes substantially to both premature skin aging and skin cancer. This can be understood in the context of studies showing that both UVA and UVB suppress the body's immune system, and that this immunosuppression plays a major role in cancer caused by ultraviolet light (Kripke 2003; Moyal and Fourtanier 2002).

There are three types of skin cancer. *Basal-cell carcinoma* (BCC) is most common, followed by *squamous-cell carcinoma* (SCC). These are together called *nonmelanoma* or *nonmelanocytic skin cancer* (NMSC). Basal-cell carcinomas can be quite invasive (Fig. 16.40) but rarely metastasize or spread to distant organs. Squamous-cell carcinomas are more prone to metastasis. *Melanomas* are much more aggressive and frequently metastasize.

Armstrong and Kricker (2001) review the epidemiology of skin cancer. There are geographic variations of *incidence*, the number of newly diagnosed cases per 100,000 population per year. Incidence in New Mexico around 1980 for the three types of skin cancer is given in Table 14.5 for Anglos and Hispanics. Their review includes ambient solar radiation, ethnic origin, color of unexposed skin, personal exposure history, and personal use of skin protection.

The International Agency for Research on Cancer (IARC 2009) has classified all UV radiation (including UVA) as "Group 1, carcinogenic to humans."

Table 14.5 Estimates of skin cancer incidence rates per 100,000 in New Mexico, about 1980. (From Fig. 3 in Armstrong and Kricker 2001)

Cancer type	Population	Males	Females
Melanoma	Anglo	11.6	11.4
	Hispanic	1.2	1.5
SCC	Anglo	143	55
	Hispanic	13	12
BCC	Anglo	495	304
	Hispanic	64	35

SCC squamous-cell carcinoma, *BCC* basal-cell carcinoma

There has been an alarming increase in the use of tanning parlors by teenagers and young adults. These emit primarily UVA, which can cause melanoma. Exposure rates are two to three times greater than solar radiation at the equator at noon (Schmidt 2012). Many states now prohibit minors from using tanning parlors. Proponents of tanning parlors point out that UVB promotes the synthesis of vitamin D; however, the exposure to UVB in a tanning parlor is much higher than needed by the body for vitamin D production. Tanning as a source of Vitamin D is no longer recommended at any age level (Barysch et al. 2010). An analysis by Lazovich et al. (2010) concludes: "our results add considerable weight to the IARC report that indoor tanning is carcinogenic in humans and should be avoided to reduce the risk of melanoma." Australia has the highest incidence of skin cancer in the world and is a leader in studying and mitigating skin cancer. A recent review by O'Sullivan and Tait (2014) makes an even stronger recommendation: "The research to date supports a complete ban of indoor tanning as it has shown that less stringent regulations are ineffective due to the lack of adherence to them and enforcement of them. Australia and New Zealand are in a powerful position to lead the developed world by imposing a complete ban on indoor tanning. It is imperative to act on this evidence to reduce the risk of further avoidable morbidity and mortality."

14.10.5 Protection From Ultraviolet Light

Protection from the sun certainly reduces erythema and probably reduces skin cancer. Protection is most important in childhood years, both because children receive three times the annual sun exposure of adults and because the skin of children is more susceptible to cancer-causing changes. The simple sun protection factor (SPF) alone is not an adequate measure of effectiveness, because it is based on erythema, which is caused mainly by UVB. Some sunscreens do not adequately protect against UVA radiation. Buka (2004) reviews both sunscreens and insect repellents for children. He finds several products that adequately block both UVA and UVB. Look for a sunscreen labeled "broad spectrum" or with at least three stars in a UVA rating system. An adequate amount must be used: for children he recommends 1 fluid ounce (30 ml) *per application* of a product with SPF of 15 or more. The desired application of sunscreen is 2 mg cm^{-2}. Typical applications are about half this amount. It has been suggested that one make two applications (Teramura et al. 2012) or use a sunscreen with a very high SPF (Hao et al. 2012).

Because of the high reflectivity of sand and snow, beach umbrellas provide at most a factor of two protection. Hats need to have a brim that is at least 7.5 cm wide (Diffey and Cheeseman 1992). Automobile window glass provides protection against UVB; however untinted glass transmits enough UVA to present a significant exposure over several hours of driving (Kimlin and Parisi 1999).

14.10.6 Ultraviolet Light Damages the Eye

The effect of ultraviolet light on the eye has been reviewed by Bergmanson and Söderberg (1995). Acute effects include *keratitis* (inflammation of the cornea, the transparent portion of the eyeball) and *conjunctivitis* (inflammation of the conjunctiva, the mucous membrane covering the eye), also known as snow blindness or welder's flash. Laboratory studies show that ultraviolet-light exposure causes thickening of the cornea and disrupts corneal metabolism. UVC radiation is absorbed by the cornea. The lens absorbs UVB and, in older persons, UVA and visible light. Only a little UVA light reaches the retina. The retina is also susceptible to trauma from blue light. Low doses cause photochemical changes in tissues, while high doses also cause thermal damage.

Chronic low exposure to ultraviolet light causes permanent damage to the cornea, known as *droplet keratopathy* or *spheroid degeneration*. UVA radiation is a significant factor in the development of a *pterygium*, a hyperplasia of the conjunctiva that may grow over the cornea and impair sight. Rarely, it causes blindness.

Properly designed spectacles and contact lenses can protect the eye against ultraviolet light (Giasson et al. 2005). However, both must be designed to absorb ultraviolet. Soft contacts are larger and provide more protection than rigid gas-permeable contacts. Protection from high-intensity ultraviolet light requires sunglasses or welding goggles. Wide-brimmed hats also help protect the eye from ultraviolet light.

14.10.7 Ultraviolet Light Therapy

Ultraviolet light is used in therapy, primarily for the treatment of a skin disease called *psoriasis*, an inflammatory disorder in which the basal cells move out to the stratum corneum in much less than the normal 28 days. The skin

is red and has thick scaling. UVB radiation, often in conjunction with coal tar applied to the skin, has been used as a treatment for psoriasis since the 1920s. In the 1960s a treatment was developed that uses UVA and a chemical either applied to the skin or administered systemically (photochemotherapy or PUVA—psoralen UVA). The chemical is a psoralen derivative. It affects DNA, and when the affected DNA is irradiated with ultraviolet light, cross-links form, preventing replication. There are well-defined guidelines for the use of PUVA to treat psoriasis (Stern 2007). PUVA therapy is also useful in cutaneous T-cell lymphoma, a disease that first becomes apparent on the skin and then moves to internal organs.

Another treatment, *extracorporeal photopheresis*, involves removing the patient's blood, extracting the red blood cells, irradiating the plasma and white blood cells with UVA light outside the body, and returning the red blood cells and the irradiated white blood cells and plasma to the patient (Grossweiner 1994, pp. 167f; Knobler et al. 2009).

14.11 Heating Tissue with Light

Sometimes tissue is irradiated in order to heat it; in other cases tissue heating is an undesired side effect of irradiation. In either case, we need to understand how the temperature changes result from the irradiation. Examples of intentional heating are *hyperthermia* (heating of tissue as part of cancer therapy) or *laser surgery* (tissue ablation[13]). Tissue is ablated when sufficient energy is deposited to vaporize the tissue. Heating may be a side effect of phototherapy.

The temperature changes are often modeled by a heat-flow equation containing a source term for the deposition of photon energy and a term representing flow of energy away from the site in warmed blood. This is one form of the *bioheat equation*, which can include additional terms in more complicated models.

The linear equation for heat conduction was mentioned as one form of the transport equation in Table 4.3:

$$j_H = -K\frac{dT}{dx},$$

with the units of the thermal conductivity K being J K^{-1} m^{-1} s^{-1}. When extended to three dimensions and combined with the equation of continuity (conservation of energy), this gives a heat-conduction equation with the same form as Fick's second law for diffusion:

$$\rho_t c_t \frac{\partial T}{\partial t} = K\nabla^2 T. \tag{14.43}$$

[13] In surgery, *ablation* means the excision or amputation of tissue.

Here ρ_t is the density of the tissue (kg m^{-3}) and c_t the tissue specific heat capacity (J K^{-1} kg^{-1}). The left-hand side of the equation is the rate of energy increase in the tissue per unit volume, and the right-hand side is the net rate of heat flow into that volume by conduction—energy flowing because warmer molecules with more kinetic energy transfer energy to cooler neighbors in a collision process analogous to a random walk. This model is for solids; in liquid one must also consider convection.

We now add a term for energy carried away by flowing blood. In the linear approximation it is proportional to the temperature difference between the tissue and the blood supply and also to the rate of blood flow. Units for this term can be quite confusing and need to be examined in detail. Blood flow is usually defined by physiologists as the *perfusion* P, which is the volume flow of blood per unit mass of tissue. The SI units for P are

$$P\,\frac{m^3\ \text{(blood)}}{\left[\text{kg (tissue)}\right]\ \text{s}}.$$

Its product with the tissue density is the volume flow of blood per unit volume of tissue:

$$\rho_t P = \frac{\left[\text{kg (tissue)}\right]\left[\text{m}^3\ \text{(blood)}\right]}{\left[\text{m}^3\ \text{(tissue)}\right]\left[\text{kg (tissue)}\right]\ \text{s}} = \frac{\text{m}^3\text{(blood)}}{\text{m}^3\text{(tissue)}\ \text{s}} = \text{s}^{-1}.$$

The quantity is analogous to clearance (Chap. 2). Its inverse is the time it takes for a volume of blood equal to the tissue volume to flow through the tissue. Each term of our heat-flow equation has units of energy per unit volume of tissue per second. If we assume that the blood enters the tissue at temperature T_0 and leaves at temperature T, the energy lost by the volume is the heat capacity of blood, c_b, times its mass per unit volume times the temperature rise. The new term in the heat-flow equation is

$$c_b\frac{\text{J}}{\text{K kg (blood)}} \times \rho_b\frac{\text{kg (blood)}}{\text{m}^3\ \text{(blood)}} \times \rho_t P\frac{\text{m}^3\ \text{(blood)}}{\text{m}^3\ \text{(tissue)}\ \text{s}} \times [(T - T_0)\ \text{K}]$$

or

$$c_b\rho_b\rho_t P(T - T_0)\frac{\text{J}}{\text{m}^3\ \text{(tissue)}\ \text{s}},$$

so the heat-flow equation with blood flow added is

$$\rho_t c_t \frac{\partial T}{\partial t} = K\nabla^2 T - c_b\rho_b\rho_t P(T - T_0).$$

The last term we consider is the energy deposited by the photon beam. In Sect. 14.6 we defined the particle fluence and particle fluence rate for photons. The definition can be used for both collimated beams and diffuse radiation. In a similar way we define the *energy fluence* Ψ as the ratio of the

expectation value of the amount of photon energy traversing a small sphere of radius a divided by the area of a great circle of the sphere, πa^2. The *energy fluence rate* is

$$\psi = \frac{d\Psi}{dt}. \tag{14.44}$$

The energy per unit volume lost by a beam with energy fluence rate ψ can be determined by the following argument. Consider only the fluence rate due to photons traveling in a certain direction. Orient the z axis in that direction and consider a small volume $dSdz$. The rate at which energy flows into the volume is ψdS, and the rate at which it is absorbed is $\psi dS\mu_a dz$. Therefore, the rate of absorption per unit volume is $\mu_a\psi$, independent of the direction the photons travel. The final heat-flow equation is

$$\rho_t c_t \frac{\partial T}{\partial t} = K\nabla^2 T - c_b\rho_b\rho_t P(T - T_0) + \mu_a\psi. \tag{14.45}$$

For monoenergetic photons, the photon energy fluence rate is related to the photon fluence rate by

$$\psi = h\nu\varphi. \tag{14.46}$$

In general, one must first solve Eq. 14.27 to determine ψ and then solve Eq. 14.45. We could add other terms, such as one for the thermal energy produced by metabolism within the tissue.

Sometimes Eq. 14.45 is written with all terms divided by $\rho_t c_t$, and sometimes with all terms divided by K. If we divide by $\rho_t c_t$, the equation is similar in form to the diffusion equation in Chap. 4:

$$\frac{\partial T}{\partial t} = D\nabla^2 T - \frac{c_b}{c_t}\rho_b P(T - T_0) + \frac{\mu_a}{\rho_t c_t}\psi, \tag{14.47}$$

where

$$D = \frac{K}{\rho_t c_t}. \tag{14.48}$$

Values of D are in the range $(0.5\text{–}2.5)\times 10^{-7}$ m^2 s^{-1} depending on the tissue type (Grossweiner 1994, pp. 127–129). We saw in Chap. 4 that for a spreading Gaussian solution to the diffusion equation the variance is $\sigma_x^2 = \sigma_y^2 = \sigma_z^2 = 2Dt$. The thermal relaxation time, that is, the average time for the temperature rise to spread a distance x, is therefore $x^2/2D$ in one dimension, $x^2/4D$ in two dimensions, and $x^2/6D$ in three dimensions.

There is an interplay between the thermal conductivity term and the blood-flow term. The *thermal penetration depth* δ_{th} is the distance at which the two terms are comparable. For larger distances blood flow is more important. To estimate the penetration depth, assume that $T - T_0$ changes over this distance. Then the Laplacian is approximated by $\nabla^2 T \approx (T - T_0)/\delta_{\text{th}}^2$. Equating the diffusive and blood flow terms gives

$$D\frac{T - T_0}{\delta_{\text{th}}^2} = \frac{c_b}{c_t}\rho_b P(T - T_0)$$

so

$$\delta_{\text{th}}^2 = D\frac{c_t}{c_b}\frac{1}{\rho_b P} = \frac{K}{\rho_t c_b \rho_b P}. \tag{14.49}$$

Grossweiner (1994) discusses values for the various tissue parameters, their temperature dependence, and simple models for tissue heating and ablation.

14.12 Radiometry and Photometry

This section develops some of the concepts and vocabulary of *radiometry*, the measurement of radiant energy. We will be considering five types of radiant energy in the remaining chapters: infrared radiation, visible light, ultraviolet radiation, x rays, and charged particles. Concepts for the measurement of radiant energy were developed simultaneously in different disciplines and even in different wavelength regions, depending on the purpose and the measurement techniques that were originally available.

It is recommended that the term *photometry* be reserved for measurement of the ability of electromagnetic radiation to produce a human visual sensation, that *radiometry* be used to describe the measurement of radiant energy independent of its effect on a particular detector, and that *actinometry* be used to denote the measurement of photon flux or photon dose (total number of photons) independent of any subsequent photoactivated process (Zalewski 2009, p. 34.10). This section reviews radiometric units and introduces a few of the related units from photometry and actinometry. Nomenclature is slightly different for x rays and charged particles.

Section 14.6 described two quantities, the photon fluence and the photon fluence rate. The energy fluence and energy fluence rate were introduced in Sect. 14.11. These are reviewed and compared here so that all the definitions are in one place. The definitions are summarized in Table 14.6. Symbols are shown for quantities used in this text. The third column shows symbols that have been recommended by the American Association of Physicists in Medicine (AAPM 57 1996). They often differ from the usage in this book.

Table 14.6 A comparison of radiometric, photometric, and actinometric quantities. Symbols are given for those quantities used in this text. The column "Symbol sometimes used" gives an alternate symbol that is often found. See, for example, *AAPM57*(1996)

Radiometric quantity	Symbol used here	Symbol sometimes used	Units	Photometric quantity	Symbol	Units	Actinometric quantity	Symbol	Units
General quantities									
Radiant energy emitted, transferred, or received	R	Q	J	*Luminous energy*	R_v	lm s	*Number of photons* emitted, transferred, or received	N	
Radiant flux: radiant power emitted, transferred, or received	P	P or Φ or $\dot{R}$	W	*Luminous flux*	P_v	lm	*Photon flux*		s^{-1}
Radiance: radiant power per unit solid angle per unit area of surface projected perpendicular to the radiant energy. It can be defined on the surface of a source or detector or at any point on the path of a ray of radiation	L	r	$W\,m^{-2}\,sr^{-1}$	*Luminance*	L_v	candela m^{-2} (cd m^{-2})	*Photon flux radiance*		m^{-2} sr^{-1}
Energy fluence: ratio of the expectation value of the radiant energy striking a small sphere to the area of a great circle of the sphere	Ψ	H_0	$J\,m^{-2}$				*Photon fluence:* ratio of expectation value of the number of photons striking a small sphere to the area of a great circle of the sphere	Φ	m^{-2}
Energy fluence rate: energy fluence per unit time	ψ	E_0	$W\,m^{-2}$				*Photon fluence rate:* photon fluence per unit time	ϕ	m^{-2} s^{-1}
Quantities emitted from a surface									
Radiant intensity: radiant power or flux emitted by a point source in a given direction per unit solid angle		I	$W\,sr^{-1}$	*Luminous intensity*		lm sr^{-1} or candela (cd)	*Photon flux intensity.*		sr^{-1}
Exitance: radiant power or flux emitted or reflected per unit area		W_r	$W\,m^{-2}$	*Luminous exitance*		lm m^{-2}	*Photon exitance*		m^{-2}
Quantities incident on a surface									
Irradiance: power per unit area incident on a surface	E	E	$W\,m^{-2}$	*Illuminance*		lm m^{-2} or lux	*Photon flux irradiance*		m^{-2} s^{-1}
Radiant exposure: radiant energy arriving per unit area		H	$J\,m^{-2}$	*Luminous exposure*		lm s m^{-2}	*Photon flux exposure*		m^{-2}

14.12.1 Radiometric Definitions

14.12.1.1 Radiant Energy and Power

The total amount of energy being considered is the *radiant energy* R, measured in joules. It can be the energy emitted by a source, transferred from one region to another, or received by a detector. We use subscripts s and d to refer to the source and detector. In optics the radiant energy is electromagnetic radiation. In radiological physics we will also consider energy transported by charged particles such as electrons and protons, and by neutral particles such as photons and neutrons.

The rate at which the energy is radiated, transferred, or received is the *radiant power* P (watts).

14.12.1.2 Point Source: Radiant Intensity

The simplest source is a point that radiates uniformly in all directions. The *radiant intensity* or radiant power per unit solid angle (Appendix A) leaving a point source radiating uniformly in all directions is

$$\frac{dP}{d\Omega} = \frac{P}{4\pi} \quad (\mathrm{W\ sr^{-1}}). \tag{14.50}$$

The power per unit area falls as $1/r^2$, while the power per unit solid angle is independent of r.[14] A point source need not radiate uniformly in all directions. For example, a searchlight 1 m in diameter viewed from a point several kilometers away appears to be a point. The light might be confined to a cone with a half-angle of 1°. Then a plot of $dP/d\Omega$ might look like Fig. 14.31. The total power radiated by the point source is

$$P = \int \frac{dP}{d\Omega}\, d\Omega. \tag{14.51}$$

If the power per unit solid angle is symmetric about the axis of the beam and θ is the angle with respect to the beam axis, then (see Appendix L)

$$P = \int_0^{\pi} \frac{dP}{d\Omega} 2\pi \sin\theta\, d\theta.$$

14.12.1.3 Extended Source: Radiance

The radiant energy leaving a source can travel in many different directions. The radiation striking a surface can come from many different directions. If we consider any small area in space there will generally be radiation passing through that area traveling in many different directions. In each case, the radiant energy or the radiant power is proportional to the magnitude of the small area projected perpendicular to the direction the energy is traveling, and to the size of the solid angle—the range of directions—being considered.

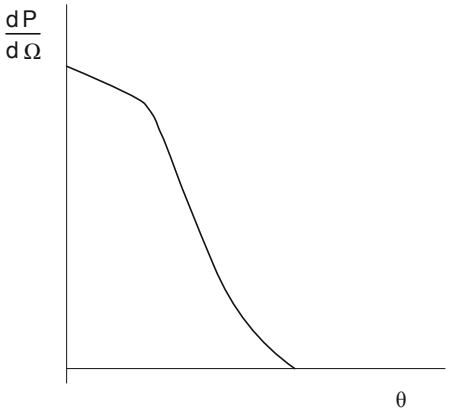

Fig. 14.31 A plot of power per unit solid angle as a function of angle from the axis of a hypothetical searchlight

The *radiance* L is the amount of radiant power per unit solid angle per unit surface area projected perpendicular to the direction of the radiant energy. The radiance of radiation traveling through a small area in space is sometimes difficult to visualize. Figures 14.32 and 14.33 may help. Figure 14.32 shows radiation leaving three points on a surface at the left. Some of it passes through the surface represented by the vertical line on the right. The energy passing through that surface has components from each point on the radiating surface. Figure 14.33 shows radiation in a very narrow cone of solid angles passing through surface dS whose normal is at an angle θ with the beam direction. The radiance is the power per unit solid angle divided by $dS\cos\theta$.

We have already seen the *energy fluence* Ψ, which is a measure of the total radiation entering or leaving a small volume of space. It is the total amount of energy striking a small sphere of radius a divided by the area of a great circle πa^2 in the limit as the radius approaches zero. Strictly speaking, if we repeat the experiment many times, the amount of energy striking the sphere fluctuates. The energy fluence is defined in terms of the expectation value of this fluctuating quantity. Figure 14.12 shows two examples. In Fig. 14.12a, a parallel beam with energy R passes through a circular area πa^2 for a time Δt. In Fig. 14.12b, a total amount of energy R strikes a sphere of radius a from many different directions. In both cases, $\Psi = R/\pi a^2$. Notice that some of the energy passing through the sphere passes outside a great circle that is not perpendicular to the direction in which the radiation is traveling, but it does pass through a great circle constructed perpendicular to its direction of travel.

[14] The lighting industry calls $dP/d\Omega$ the intensity, while in physical optics intensity is used for power per unit area. We will try to avoid using the word intensity alone.

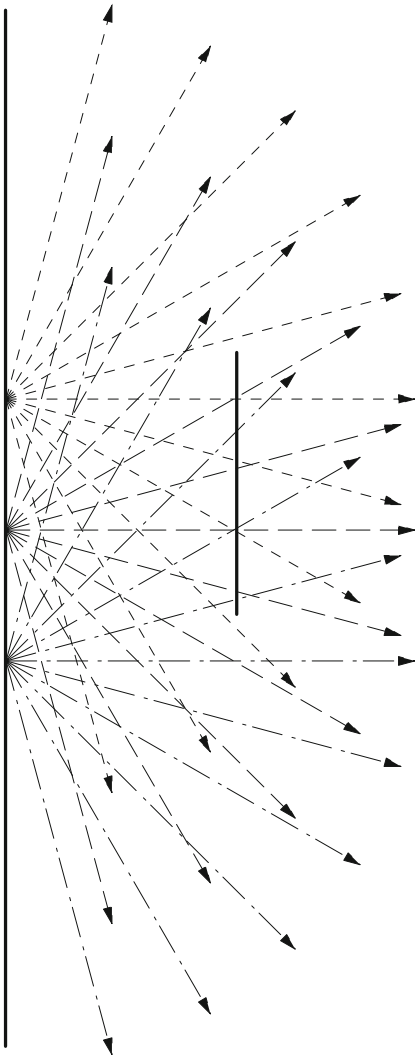

Fig. 14.32 Radiation emitted from different points of the surface on the left strikes the surface on the right

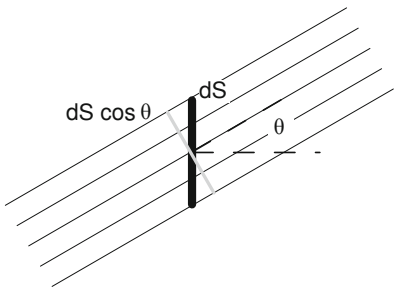

Fig. 14.33 Surface area dS, projected perpendicular to the direction of the radiation, has projected area $dS\cos\theta$

The *energy fluence rate* is the amount of energy fluence per unit time (which for the small sphere is $P/\pi a^2$):

$$\psi = \frac{d\Psi}{dt}. \tag{14.52}$$

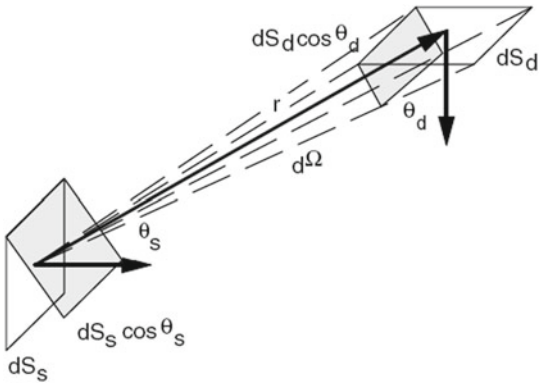

Fig. 14.34 Radiant energy is emitted from a source of surface area dS_s into a cone of solid angle $d\Omega$. The direction of emission is at an angle θ_s with the normal to the surface. A detecting surface has an element of area dS_d oriented at a direction θ_d to the direction of travel of the radiation from source to detector. The shaded rectangles show the projections of dS_s and dS_d perpendicular to the line of length r from source to detector

The *exitance* W_r is the radiant power or flux emitted per unit area of a surface.

14.12.1.4 Energy Striking a Surface: Irradiance

Now consider the energy striking a surface. The *irradiance* E is the power per unit area incident on a surface. The strict definition is the ratio of the power incident on an infinitesimal element of detector surface dS_d to the area projected perpendicular to the direction the radiant energy is traveling. If θ_d is the angle between a normal to the surface and the direction of propagation, the irradiance is

$$E = \frac{1}{\cos\theta_d}\frac{dP}{dS_d}. \tag{14.53}$$

For a point source radiating uniformly in all directions, the power at distance r is spread uniformly over a sphere of area $4\pi r^2$, so the irradiance on a detecting surface perpendicular to a line back to the source is

$$E = \frac{P}{4\pi r^2} \qquad \text{(isotropic point source)}. \tag{14.54}$$

For an extended source the power emitted by the surface is proportional to both the size of the emitting area dS_s and the solid angle of the cone $d\Omega$ into which the energy is radiated, as shown in Fig. 14.34. The solid angle subtended by a small element of area on the detector is $d\Omega$, as shown by the dashed lines. The amount of power radiated into $d\Omega$ from dS_s is

$$L dS_s d\Omega = \frac{1}{\cos\theta_s}\frac{d^2P}{dS_s\, d\Omega} dS_s\, d\Omega, \tag{14.55}$$

where the radiance L depends on the direction of emission as well as the location on the surface. This equation is valid

whether the energy is emitted directly from the source (as in a glowing object) or is scattered by the surface (as from this page). The total power emitted is

$$P = \int\int L\, dS_s\, d\Omega. \tag{14.56}$$

The distinction between angles and areas for the source and the detector is shown in Fig. 14.34. Note that the solid angle subtended at the source by dS_d is $d\Omega = dS_d \cos\theta_d / r^2$. The power into an area dS_d of the detector from area dS_s of the source is therefore

$$d^2P = \frac{L \cos\theta_s \cos\theta_d\, dS_s\, dS_d}{r^2}. \tag{14.57}$$

14.12.1.5 Plane-Wave Relationships

We can derive some useful relationships for a beam of collimated radiation all traveling in one direction (a *plane wave*). Imagine that the collimated beam comes from a distant point source radiating power P. The energy fluence rate at distance r from the source is the power through a sphere of radius a divided by πa^2:

$$\psi = \frac{\pi a^2 P}{4\pi r^2}\frac{1}{\pi a^2} = \frac{P}{4\pi r^2}.$$

This is also the power per unit area incident on a circle of radius a oriented perpendicular to the beam. Therefore, for a collimated beam,

$$\psi = E \quad \text{(collimated beam)}. \tag{14.58}$$

14.12.1.6 Isotropic Radiation: Lambert's Law

In general, L may depend on the angle of emission. In some cases, such as reflection from a "perfectly diffuse" surface, the radiation is isotropic : $L = L_0$. This is called *Lambert's law of illumination* or Lambert's cosine law.[15]

A surface described by Lambert's law will have equal power per unit area in the image regardless of the viewing angle. Look at surfaces around you. Do similar surfaces illuminated the same way appear to have the same brightness when they are oblique to your line of vision?

The power incident on a small element of surface area dS_d from angle $d\Omega$ is $L_0 dS_d \cos\theta_d\, d\Omega$, where θ_d is the angle that the incident radiation makes with the normal to the surface. The solid angle is $2\pi \sin\theta_d\, d\theta_d$ (see Fig. 14.11b). The irradiance is

$$E = \frac{dS_d 2\pi L_0 \int_0^{\pi/2} \cos\theta_d \sin\theta_d d\theta_d}{dS_d} = \pi L_0. \tag{14.59}$$

[15] Sometimes Eq. 14.57 is defined without the factor $\cos\theta_s$, in which case Lambert's law has the form $L(\theta_s) = L_0 \cos\theta_s$.

The same geometry is used with dS_s to show that for isotropic radiation, the exitance is

$$W_r = \pi L_0. \tag{14.60}$$

To determine the energy fluence rate for isotropic radiation consider a small sphere of radius a and the radiation arriving in a small solid angle $d\Omega$ about a line perpendicular to a great circle of the sphere. The power is $L_0 \pi a^2 d\Omega$. This argument applies for any direction of the radiation. Integrating over all directions gives the total power $L_0 \pi a^2 4\pi$. Therefore, for isotropic (Lambertian) radiation,

$$\psi = 4\pi L_0 = 4E \quad \text{(isotropic radiation)}. \tag{14.61}$$

14.12.1.7 The Spectrum

When the energy is not monochromatic, we define the amount of energy per unit wavelength interval as R_λ, with units J m^{-1} or J nm^{-1}. The total energy between wavelengths λ_1 and λ_2 is

$$\int_{\lambda_1}^{\lambda_2} R_\lambda(\lambda)\, d\lambda \tag{14.62a}$$

and between frequencies ν_1 and ν_2 it is

$$\int_{\nu_1}^{\nu_2} R_\nu(\nu) d\nu. \tag{14.62b}$$

The relationship between R_λ and R_ν is the same as in Eqs. 14.36 and 14.37.

14.12.2 Photometric Definitions

For the photometric units we also need to know the sensitivity of the eye. The eye contains two types of light receptors: *rods*, which have no color discrimination but are most sensitive, and *cones*, which are less sensitive and can discriminate color. *Photopic* vision is normal vision at high levels of illumination in which the eye can distinguish colors. *Scotopic* vision occurs at low light levels with a dark-adapted eye. The CIE has established the spectral efficiency function V for the eye of a standard observer for both photopic vision $[V(\lambda)]$ and scotopic vision $[V'(\lambda)]$. Both are normalized to unity at their peak (Fig. 14.35).

The *luminous flux* P_v in lumens (lm) is the analog of the energy flux P. The peak sensitivity for photopic vision is for green light, $\lambda = 555$ nm. At that wavelength the relationship between P and P_v is

$$\begin{aligned} P = 1\,\text{W} &\Longleftrightarrow P_v = 683\,\text{lm}, \\ P_v = 1\,\text{lm} &\Longleftrightarrow P = 1.464 \times 10^{-3}\,\text{W}. \end{aligned} \tag{14.63a}$$

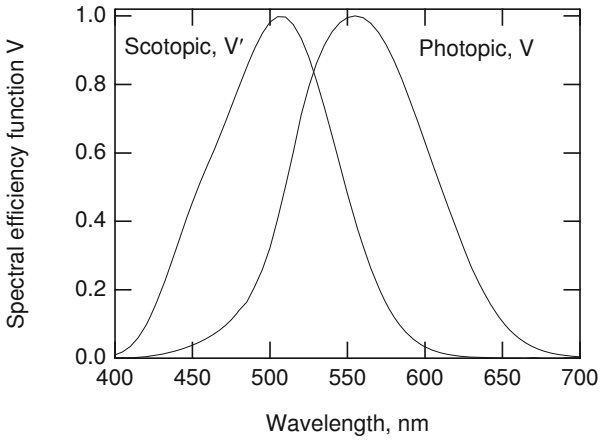

Fig. 14.35 The spectral efficiency functions for the CIE standard eye. Plotted from data in Table 2 of Zalewski (2009)

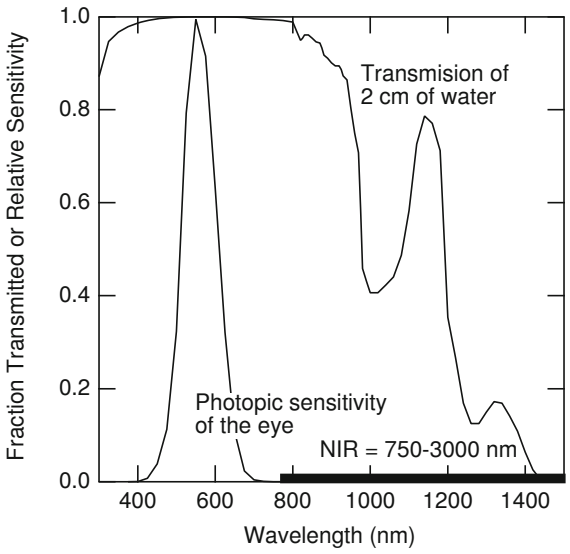

Fig. 14.36 Transmission of light through 2 cm of water, compared to the spectral efficiency of the eye

The ratio P_v/P at 555 nm is the *luminous efficacy* for photopic vision, $K_m = 683$ lm W^{-1}. For a distribution of wavelengths,

$$P_v(\text{photopic}) = K_m \int_{400\text{ nm}}^{700\text{ nm}} V(\lambda) P_\lambda(\lambda)\, d\lambda. \qquad (14.63b)$$

An analogous relationship holds for scotopic vision, with $K'_m \approx 1700$ lm W^{-1}:

$$P_v(\text{scotopic}) = K'_m \int_{400\text{ nm}}^{700\text{ nm}} V'(\lambda) P_\lambda(\lambda)\, d\lambda. \qquad (14.63c)$$

If P were spread uniformly over the visible spectrum, the overall conversion efficiency would be about 200 lm W^{-1}. A typical incandescent lamp has an efficiency of 10–20 lm W^{-1}, while a fluorescent lamp has an efficiency of 60–80 lm W^{-1}. A typical LED replacment lamp is about 75 lm W^{-1}. The number of lumens per steradian is the *luminous intensity*, in lm sr^{-1}. The lumen per steradian is also called the *candela*. Other units are shown in Table 14.6.

The peak of the eye's spectral efficiency function is at about the peak of the sun's blackbody spectrum when plotted as a function of wavelength (Eq. 14.33). Some authors have speculated that this is because we evolved in sunlight. There is a severe problem with this argument. The spectral efficiency function has the same value whether we consider a particular wavelength or its corresponding frequency. The blackbody spectrum is a distribution function—per wavelength interval (Eq. 14.33) or per frequency interval (Eq. 14.38).[16] The sun's blackbody spectrum plotted versus frequency peaks at a frequency corresponding to a wavelength of 880 nm, far from the peak of the spectral efficiency function (See Fig. 14.24). Soffer and Lynch (1999) have discussed this at length and describe several of the errors in the literature. The structures in the human eye, as in all vertebrate eyes, are mostly water. All vertebrate eyes are sensitive between 390 and 760 μm, with a peak at 500–550 μm. It is interesting to compare the spectral efficiency function with the transmission of light through 2 cm of water (Fig. 14.36). The eye's response is pretty well centered in this absorption window. Many insects, crustaceans, fish, birds, and reptiles have ultraviolet-sensitive receptors (Kevan et al. 2001).

14.12.3 Actinometric Definitions

The actinometric quantities count the number of photons. For monochromatic photons the energy is the number of photons times $h\nu$. Therefore an actinometric quantity is easily obtained when the radiometric quantity is known. The units are shown in Table 14.6.

14.13 The Eye

This section presents a simple model for the eye, sufficient for us to understand how refractive errors are corrected and to see how photons strike the retina, so that the sensitivity of the eye can be determined in the next section. For a detailed but nonmathematical introduction to the eye and vision, see Rodieck (1998).

[16] Other distribution functions are also useful, for example, per logarithmic frequency or wavelength interval. See Soffer and Lynch (1999) or Heald (2003).

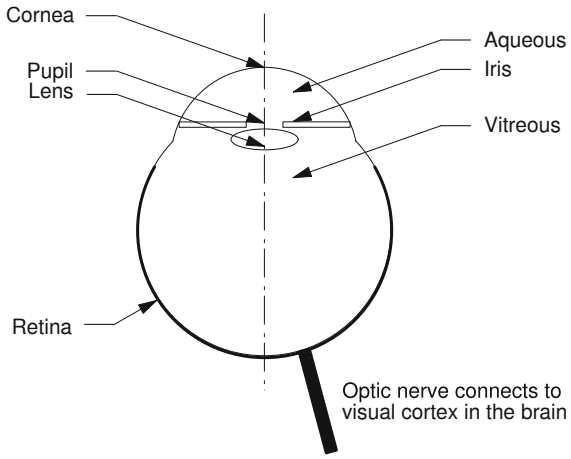

Fig. 14.37 A simplified cross section of the left eye, viewed from above

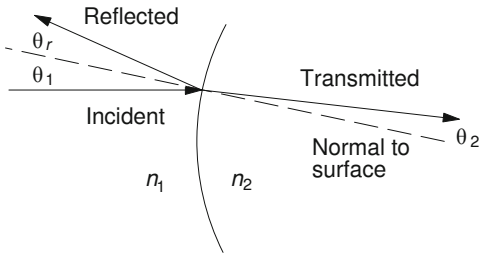

$$n_1 \sin\theta_1 = n_2 \sin\theta_2$$

$$\theta_1 = \theta_r$$

Fig. 14.38 Light passing from one medium to another with a different index of refraction. All angles are measured with respect to the normal to the surface

A simplified cross section of the eye is shown in Fig. 14.37. The principal components through which the light passes are the curved, thin, transparent *cornea*, the *aqueous*, the *lens*, the *vitreous*, and the *retina*. The *iris* defines the area of the *pupil*, the opening in front of the lens through which light passes.

When light passes through a surface from one medium to another, part is reflected and part is transmitted. The transmitted light usually changes direction, a process called *refraction*. Figure 14.38 shows the angles involved, all measured with respect to the dashed line, which is normal to the surface at the point where the light ray strikes. The angle the reflected light makes with the normal is the same as the angle of incidence, $\theta_r = \theta_1$. The direction the refracted light travels is described by *Snell's law*, $n_1 \sin\theta_1 = n_2 \sin\theta_2$.

When light from an object strikes the eye, it must be refracted to form an image on the retina. Most of the refraction takes place at the surface between the air and the cornea.

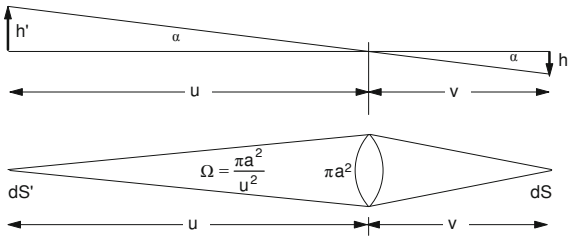

Fig. 14.39 A source of height h' emits light in all directions. Some of this light is intercepted by a lens and focused in an image. **a** Relation between object and image distances and sizes. **b** Collection of light by the lens

The cornea is very thin, and a light ray is deflected only a very small distance before it strikes the aqueous. Thus, most of the refraction occurs because of the difference between the index of refraction of the air ($n = 1.00$) and the aqueous ($n = 1.33$). The light then passes through the lens ($n = 1.42$) and the vitreous ($n = 1.33$). The lens changes shape to provide the adjustable part of the overall refraction.

A number of models at varying levels of sophistication are used to describe the formation of the image on the retina. The most detailed take into account the refraction at each surface where the index of refraction changes, including variations in different layers of the lens itself. Others treat only the refraction at the air–cornea, aqueous–lens, and lens–vitreous interfaces. The simplest model, and the one we will use, treats the eye as a thin lens of adjustable focal length f, with object distance u and fixed image distance v, as shown in Fig. 14.39. The object and image distances and focal length are related by the *thin-lens equation*:

$$\frac{1}{u} + \frac{1}{v} = \frac{1}{f}. \tag{14.64}$$

When the object is infinitely far away the image distance is equal to the focal length of the lens, $v = f$. A typical value for v is 1.7 cm. As the object is brought closer to the eye v cannot change, but the lens changes to decrease the focal length.

In ophthalmology and optometry it is customary to describe the refraction of the eye in terms of the *vergence*. When light rays are emanating from a point they are diverging, and the vergence is negative. When they are coming toward a point the vergence is positive and they are converging. When they are parallel, the vergence is zero. Quantitatively, the vergences for the geometry shown in Fig. 14.39 are

$$\begin{aligned} U &= -\frac{1}{u} \quad \text{(diverging from the object)}, \\ V &= \frac{1}{v} \quad \text{(converging to the image)}, \\ F &= \frac{1}{f} \quad \text{(a converging lens)}. \end{aligned} \tag{14.65}$$

Table 14.7 Convergence power of the eye in diopters

Refracting structure	Relaxed normal eye	Most converging eye (age 25)
Air-cornea surface	45	45
Lens	14	24
Entire eye	59	69

The relationship between the vergences is

$$V = F + U. \tag{14.66}$$

When the distances are in meters, the vergences are in *diopters*.

A given eye requires a particular value of V to form the image on the retina. The converging power of all the refracting surfaces in the eye must be $F = V$ in order to focus on an object infinitely far away. Closer objects require more convergence from the eye, which is provided by the lens. Table 14.7 shows typical values for the converging power of the eye. Most of the convergence is provided by the front surface. When the eye is relaxed, $F = V = 59$ diopters, $U = 0$, and the eye is focused on an object infinitely far away. With $F = 69$ diopters, $U = 10$, and the eye is focused on an object 0.1 m away. This ability of the lens to change shape and provide additional converging power is called *accommodation*.

In the normal or *emmetropic* eye, the length of the eye is such that when the lens is relaxed, rays with no vergence (parallel rays from a source infinitely far away) are focused on the retina ($V = F$).

In farsightedness or *hyperopia*, parallel rays come to a focus behind the retina. The relaxed eye does not have enough converging power ($F < V$). The subject can focus on distant objects by providing some additional converging power from the lens, but then the lens cannot provide enough converging power to focus on nearby objects. A corrective lens, either spectacles or a contact lens, provides additional convergence.

In nearsightedness or *myopia*, parallel rays come to a focus in front of the retina. The eye is slightly too long for the shape of the cornea ($F > V$). The total converging power of the eye is too great, and the relaxed eye focuses at some closer distance, from which the rays are diverging. Accommodation can only increase the converging power of the eye, not decrease it, so the unassisted myopic eye cannot focus on distant objects. Myopia can be corrected by placing a diverging spectacle or contact lens in front of the eye, so that incoming parallel rays are diverging when they strike the cornea.

When the eye is not symmetric about an axis through the center of the lens, the images from objects oriented at different angles in the plane perpendicular to the axis form at different distances from the lens. This is called *astigmatism*, and it can be corrected with a spectacle lens that is not symmetric about the axis. The lack of symmetry usually occurs at the surface of the cornea, so a contact lens can restore the symmetry.

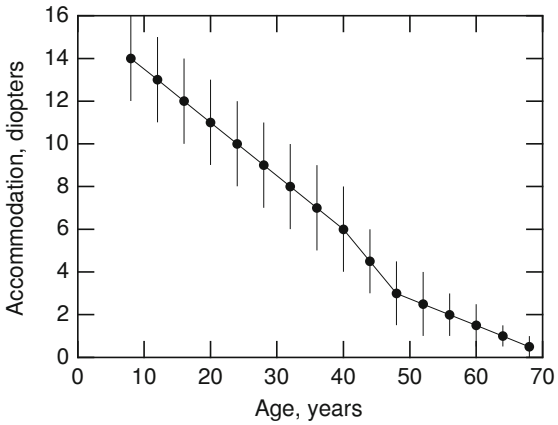

Fig. 14.40 Accommodation versus age. There is considerable variation between individuals, shown by the *error bars*

Surgery to change the radius of curvature of the cornea can also be used to correct errors of refraction.

As we age, the accommodation of the eye decreases, as shown in Fig. 14.40. A normal viewing distance of 25 cm or less requires 4 diopters or more of accommodation. The graph shows that this limit is usually reached in the early 40s. To make up for the lack of accommodation, one can place a converging lens in front of the eye when viewing nearby objects (reading glasses). Bifocals provide a different amount of convergence at the top and bottom of the lens. This can be done either by grinding the lower portion of the lens with a different radius of curvature or by fusing glass with a different index of refraction into the lens.

The sharpness of the image is reduced by two other effects: *chromatic aberration* and *spherical aberration*. Chromatic aberration occurs because the index of refraction varies with wavelength. There is nearly a 2-diopter change in overall refractive power from the red to the blue. Spherical aberration occurs because the refractive power changes with distance from the axis of the eye. This is different from astigmatism, which is a departure from symmetry at different angles about the axis.

A concept important in both vision and photography is *depth of field*. The retina has a finite spatial resolution, so the image of a point still appears sharp, even if it is slightly out of focus. Consider Fig. 14.41. The retina is behind the plane in which the image is in focus. In dim light, the pupil of the eye is fully open and light from a point object is spread out over the larger circle on the retina defined by the solid rays. In brighter light the pupil is smaller, and light from the same point object is confined to the smaller circle defined by the

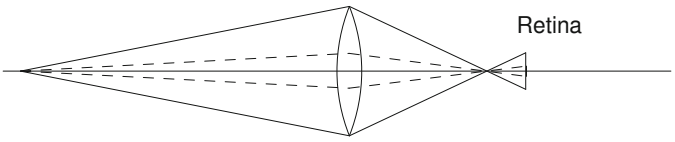

Fig. 14.41 Depth of field is illustrated by this ray diagram. The retina is slightly behind the plane of focus. In dim light, the pupil of the eye is fully open and light from a point object is spread out over the larger circle on the retina. When the light is brighter and the pupil is smaller, light from the same point object is confined to the smaller circle defined by the *dashed lines*

dashed lines. As long as this circle is smaller than the spatial resolution, the image is sharp. This is why we can see better in brighter light. An older person whose accommodation is less and who is trying to avoid bifocals often finds that bright light makes it easier to see nearby objects.

Point-spread functions and modulation transfer functions can be used to describe the image. (See, for example, Charman (2009) or Greivenkamp et al. (1995).) A simpler model describes the image by a Gaussian with a certain standard deviation, equal to the square root of the sum of the variances due to various effects. The maximum photopic (bright-light) resolution of the eye is limited by four effects: diffraction of the light passing through the circular aperture of the pupil (5–8 μm), spacing of the receptors (≈ 3 μm), chromatic and spherical aberrations (10–20 μm), and noise in eyeball aim (a few micrometers) (Stark and Theodoridis 1973). The total standard deviation is $(6^2+3^2+15^2+5^2)^{1/2} = 17$ μm in the image on the retina. Since the diameter of the eyeball is about 2 cm, this corresponds to an angular size (α in Fig. 14.39) of $(17 \times 10^{-6})/(2 \times 10^{-2}) = 8.5 \times 10^{-4}$ rad $= 0.048^\circ =$ 2.9 min of arc. (For further discussion, see Cornsweet (1970, Chap. 3).)

14.14 Quantum Effects in Dark-Adapted Vision

The visual process involves two steps. First, the eye creates an image of an external object on the retina as described above. Then the photon stimulus is transduced into neurological signals that are interpreted by the central nervous system. The discussion here is limited to a classic experiment on scotopic vision that shows the importance of quantum effects (shot noise) in human vision in dim light. For a more detailed discussion of how photoreceptors detect photons, see Rodieck (1998).

The experiment was performed by Hecht, Shlaer, and Pirenne in 1942. It has been described in many places. A detailed nonmathematical description is that by Cornsweet (1970).

The retina can be divided into two regions. The *fovea*, the area of greatest visual discrimination, is composed entirely

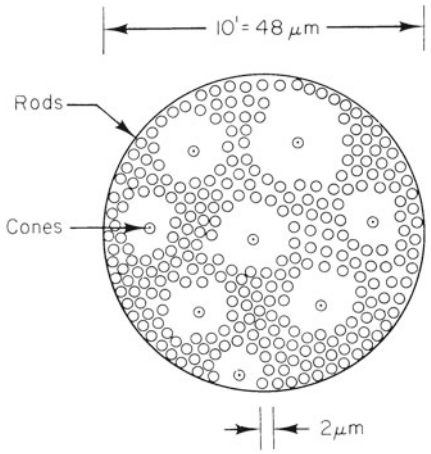

Fig. 14.42 An example of a 10-minute-of-arc field superimposed on the rods and cones in the retina in the region of greatest sensitivity

of cones. The percentage of rods is highest a few millimeters away from the fovea, and this part of the retina is most sensitive to faint light. The dark-adapted eye increases sensitivity by a factor of about 5000.

The experiment was done by having the subject look directly at a very dim red fixation point while a green light was flashed in such a place that its image fell on the most sensitive part of the retina. Experiments on the sensitivity of the dark-adapted eye to flashes of weak light have shown that if the flash duration is less than 100 ms and the light on the retina covers a *receptor field* less than 10 min of arc in size, the scotopic response of the eye depends on the total amount of energy or the total number of photons in the flash. Photons striking anywhere within the receptor field during this time have the same effect; the eye must combine the effects occurring in all receptors in the receptor field in a tenth of a second. A scotopic receptor field is shown in Fig. 14.42. This scotopic field size (10 min of arc) cannot be compared to the 2.9 min for maximum resolution, which is for photopic vision on a different part of the retina.

In the Hecht–Shlaer–Pirenne experiment, the flashes were short enough and small enough so that only the total number of photons was important. The fraction of flashes that the subject recognized was measured as a function of the total flash energy. A typical response curve is shown in Fig. 14.43. Let q be the number of photons striking the cornea in front of the pupil in each flash, which is the total energy in the flash divided by the energy of each photon. For the 510-nm green light used, the photon energy is $hc/\lambda = 3.89 \times 10^{-19}$ J. The number of photons striking the cornea can be determined as follows. Let Lt be the radiance times the duration of the flash. Consider Eq. 14.57 with both θ_s and θ_d nearly zero. Refer also to the lower half of Fig. 14.39. The energy striking

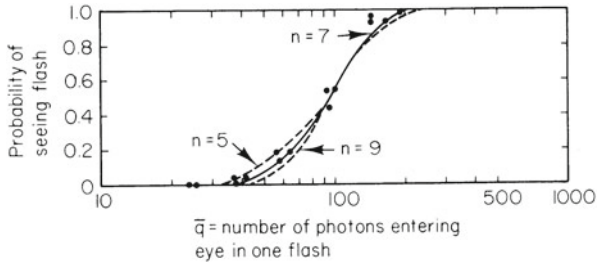

Fig. 14.43 Typical response in the experiments of Hecht, Shlaer, and Pirenne. Curves are calculated using Eq. 14.69. (Data are from Hecht et al. (1942))

the cornea over the pupil area is

$$\frac{(Lt)\,dS_s dS_d}{r^2} = \frac{(Lt)\,dS'\left(\pi a^2\right)}{u^2}.$$

Because $h = h'v/u$, the area on the retina where photons from dS' fall is $dS = dS'(v/u)^2$. The number of photons striking the cornea that would be in dS if there were no losses is

$$q = \frac{(Lt)(\pi a^2)dS'}{hvu^2} = \frac{(Lt)(\pi a^2)\,dS}{hvv^2}. \tag{14.67}$$

The number of photons fluctuates from flash to flash. Therefore we should speak of $\overline{q}$, the average number of photons striking the cornea per flash. Of these, only some fraction f actually reach the retina and are absorbed by a visual pigment molecule. The average number absorbed is

$$m = f\overline{q}. \tag{14.68}$$

Let us next postulate that some minimum number of quanta n must be absorbed during the flash in order for the subject to see it. If the average number absorbed per flash is m, there will sometimes be more and sometimes less than n photons absorbed per flash. The probability of absorbing x photons per flash is given by the Poisson distribution $P(x; m)$ (Appendix J). The probability of seeing the flash is the probability that x is greater than or equal to n :

$$\begin{aligned} P(\text{seeing}) &= \sum_{x=n}^{\infty} P(x;m) = 1 - \sum_{x=0}^{n-1} P(x;m) \\ &= 1 - e^{-m}\left(1 + m + \frac{m^2}{2!} + \cdots + \frac{m^{n-1}}{(n-1)!}\right). \end{aligned} \tag{14.69}$$

This function is plotted in Fig. 14.44 as a function of m for various values of n, with both a linear and a logarithmic scale for m.

Hecht, Shlaer, and Pirenne used an ingenious method to determine n. They plotted their data versus the logarithm of $\overline{q}$. Since $m = f\overline{q}$, $\log m = \log f + \log \overline{q}$; different values

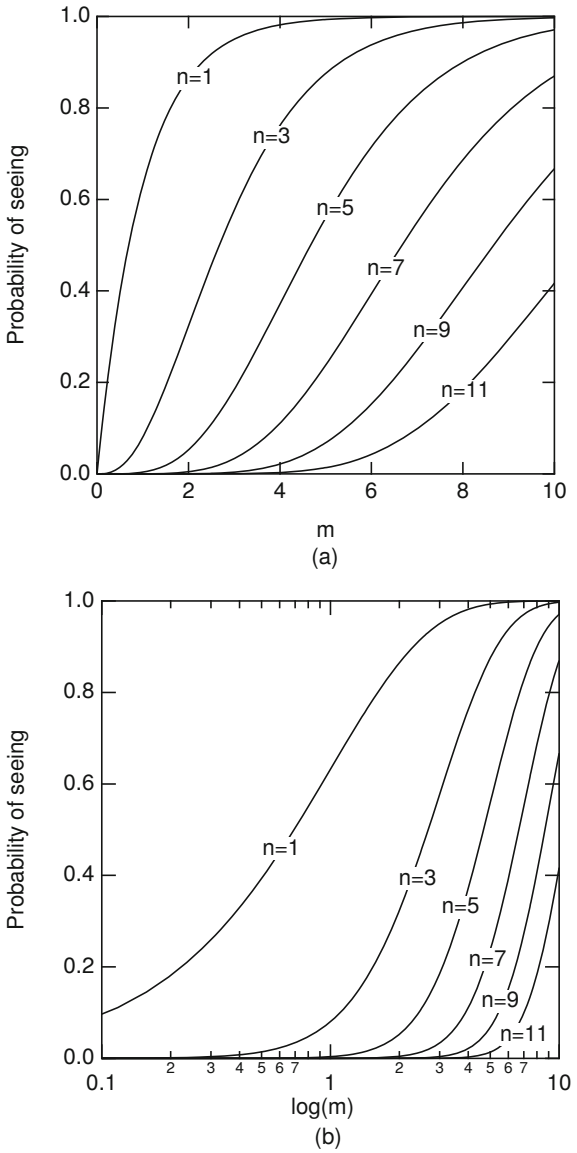

Fig. 14.44 The probability of seeing a flash, plotted versus **a** m; **b** $\log m$

of f correspond to shifting the curve along the axis. They then compared the experimental data to various theoretical curves for the probability of seeing a flash, plotted against $\log m$. Sliding the paper containing the data along the $\log m$ axis is equivalent to trying different values of f. The data in Fig. 14.43 are shown along with the curves for $n = 5$, 7, and 9. For these data, $n = 7$ gives the best fit. From Fig. 14.43, a 55% chance of detecting the flash corresponds to 100 photons for $\overline{q}$ while being consistent with $m = 7$. Therefore, $f = 0.07$.

Hecht, Shlaer, and Pirenne deduced that about seven photons must be absorbed by the rods in the area of integration shown in Fig. 14.42 within 0.1 s in order for the brain to

detect the flash of light. Their data were consistent with the hypothesis that the photons arrived at random, with the actual number in each flash obeying a Poisson distribution. Later work by Sakitt (1972) is consistent with the rods counting individual photons, with false positives produced by thermal noise within the retina (Barlow 1956).

The phototransduction mechanism is quite complicated. Rieke and Baylor (1998) reviewed the detection of photons by rod cells. When stimulated with dim light pulses, the rod cell responds to each flash consistent with the absorption of 0, 1 or, 2 photons. The rods have a dark current that is reduced when light falls on them. In other words, the light hyperpolarizes the cell. This lowers the rate of release of cyclic GMP. The review discusses what is known about the chemical transduction process.

If the light intensity is increased, m increases. There will be shot-noise fluctuations with a standard deviation equal to $m^{1/2}$, and the eye should be unable to detect brightness changes smaller than this. Measurements by Horace Barlow in 1956 showed that as long as short flashes spanning only one visual field are used, the minimum detectable intensity depends on the square root of the light intensity. This statistical limit to detecting intensity changes is a lower limit; for larger sources and longer exposure times, the minimum detectable brightness change is larger and is more nearly proportional to the intensity than to the square root of the intensity (Rose 1973).

14.15 Color Vision

The eye can detect color because there are three types of cones in the retina, each of which responds to a different wavelength of light (*trichromate vision*): red, green, and blue, the primary colors. However, the response curve for each type of cone is broad, and there is overlap between them (particularly the green and red cones). The eye responds to yellow light by activating both the red and green cones. Exactly the same response occurs if the eye sees a mixture of red and green light. Thus, we can say that red plus green equals yellow. Similarly, the color cyan corresponds to activation of both the green and blue cones, caused either by a monochromatic beam of cyan light or a mixture of green and blue light. The eye perceives the color magenta when the red and blue cones are activated but the green is not. Interestingly, no single wavelength of light can do this, so there is no such thing as a monochromatic beam of magenta light; it can only be produced my mixing red and blue. Mixing all three colors, red and green and blue, gives white light. Color printers are based on the colors yellow, cyan, and magenta, because when we view the printed page, we are looking at the reflection after some light has been absorbed by the ink. For instance, if white light is incident on a page containing ink that absorbs blue light, the reflected light will contain red and green and therefore appear yellow. Human vision is trichromate, but other animals (such as the dog) have only two types of cones (*dichromate vision*), and still others have more than three types.

Some people suffer from color blindness. The most common case is when the cones responding to green light are defective, so that red, yellow, and green light all activate only the red receptor. Such persons are said to be red–green color blind: they cannot distinguish red, yellow, and green, but they can distinguish red from blue.

As with pitch perception, the sensation of color involves both physics and physiology. For instance, one can stare at a blue screen until the cones responding to blue become fatigued, and then immediately stare at a white screen and see a yellow afterimage. Many other optical illusions with color are possible.

Symbols Used in Chapter 14

Symbol	Use	Units	First used page
a	Radius	m	390
c	Speed of light in a vacuum	$\mathrm{m\,s^{-1}}$	381
c_n	Speed of light in a medium	$\mathrm{m\,s^{-1}}$	381
c_b, c_t	Specific heat of blood, tissue	$\mathrm{J\,kg^{-1}\,K^{-1}}$	404
e	extinction coefficient	m^2	417
e	Charge on an electron	C	383
f	Focal length	m	411
f	Fraction of photons reaching retina		414
g	Scattering anisotropy factor		389
h	Planck's constant	J s	382
h, h'	Image height, object height	m	411
$\hbar$	Planck's constant divided by 2π	J s	382
i	Label of energy level		383
j	Total angular momentum quantum number		384
j_H	Energy transport in heat flow	$\mathrm{W\,m^{-2}}$	404
k	Spring constant	$\mathrm{N\,m^{-1}}$	386
k_B	Boltzmann constant	$\mathrm{J\,K^{-1}}$	395
l	Orbital angular momentum quantum number		383
m	Mass	kg	385
m	Average number		414
m_e	Mass of electron	kg	383
m_i	Mass of ith particle	kg	385
m_j, m_l, m_s	z quantum number for angular momentum		383
n	Index of refraction		381
n	Principal quantum number		383

$\overline{n}$	Average number of photons that interact		388
n	Minimum number of photons to trigger a response		414
p	Probability		389
q	Electric charge	C	382
q	Number of photons		414
$\overline{q}$	Average value of q		414
r	Rotational quantum number		385
r, $\mathbf{r}$	Coordinate	m	385
s	Spin quantum number		383
s	Source term in diffusion equation	$m^{-3}\,s^{-1}$	390
t	Time	s	382
$\mathbf{v}$	Velocity	$m\,s^{-1}$	382
v	Vibrational quantum number		386
u, v	Object and image distances	m	411
w_{tot}	Net power radiated	W	398
x, z	Distance	m	382
z_0	Depth of first scattering	m	391
A	Amplitude of wave		392
A	Molar mass	kg	388
$\mathbf{B}$	Magnetic field	T	382
C	Concentration	m^{-3}	390
D	Diffusion constant	$m^2\,s^{-1}$	390
D'	Photon diffusion constant	m	390
D	Thermal diffusion constant	$m^2\,s^{-1}$	405
$\mathbf{E}$	Electric field	$V\,m^{-1}$	382
E	Energy	J	382
E_p	Potential energy	J	386
E_r	Rotational energy	J	385
E_v	Vibrational energy	J	386
E	Irradiance	$W\,m^{-2}$	409
F, $\mathbf{F}$	Force	N	382
F	Converging power of a lens	diopter (m^{-1})	411
I	Moment of inertia	$kg\,m^2$	385
K	Thermal conductivity	$W\,K^{-1}\,m^{-1}$	404
K_m	Luminous efficiency, photopic	$lm\,W^{-1}$	410
K'_m	Luminous efficiency, scotopic	$lm\,W^{-1}$	410
L	Angular momentum	$kg\,m^2\,s^{-1}$	385
L	Radiance	$W\,m^{-2}\,sr^{-1}$	409
N	Number of photons		387
N_a	Number absorbed		387
N_s	Number scattered		387
N_A	Avogadro's number		388
N_T	Number of target entities per unit area	m^{-2}	388
P	Probability		395
P	Tissue perfusion	$m^3\,kg^{-1}\,s^{-1}$	404
P	Radiant power	W	407
P_v	Luminous flux	lm	410
Q	Rate of production	$m^{-3}\,s^{-1}$	390
R, $\mathbf{R}$	Coordinate of atom, distance	m	385
R_λ	Radiant energy per unit wavelength interval	$J\,m^{-1}$ or $J\,nm^{-1}$	409
R	Reflected fluence rate	$m^2\,s^{-1}$	391
R	Radiant energy	J	407
R	Rydberg constant	$m-1$	417
S, S'	Surface area	m^2	388
T	Period	s	382
T	Kinetic energy	J	385
T, T_s, T_o	Temperature	K	395
U	Object vergence	diopter (m^{-1})	411
V, $\mathbf{V}$	Velocity	$m\,s^{-1}$	385
V	Photopic spectral efficiency function		409
V'	Scotopic spectral efficiency function		409
V	Image vergence	diopter (m^{-1})	411
W_λ	Blackbody radiation function	$W\,m^{-3}$ or $W\,m^{-2}\,nm^{-1}$	396
W_ν	Blackbody radiation function	$W\,m^{-2}\,Hz^{-1}$	397
W_r	Exitance	$W\,m^{-2}$	408
α	Angle		411
δ_{th}	Thermal penetration depth	m	405
ϵ_0	Electrical permittivity of free space	$N^{-1}\,C^2\,m^{-2}$	382
ϵ	Emissivity		395
$\epsilon(\lambda)$	Erythema action spectrum		402
θ, ϕ	Angles		388
φ	Particle fluence rate	$m^{-2}\,s^{-1}$	390
λ	Wavelength	m	382
μ	Total linear attenuation coefficient	m^{-1}	387
μ_a	Linear absorption coefficient	m^{-1}	387
μ_s	Linear scattering coefficient	m^{-1}	387
μ'_s	Reduced linear scattering coefficient	m^{-1}	389
μ_{eff}	Effective linear attenuation coefficient	m^{-1}	391
μ_0	Magnetic permeability of free space	$\Omega\,s\,m^{-1}$	382
ρ, ρ_b, ρ_t	Density, density of blood, density of tissue	$kg\,m^{-3}$	388
σ, σ_i, σ_a, σ_s, σ_{tot}	Cross section	m^2	388
$\sigma(\theta)$, $d\sigma/d\Omega$	Differential scattering cross section	$m^2\,sr^{-1}$	388
σ_{SB}	Stefan–Boltzmann constant	$W\,m^{-2}\,K^{-4}$	397
σ_x^2, σ_y^2, σ_z^2	Variance for diffusion or heat flow	m^2	405
ν	Frequency	s^{-1}	382
τ_{coh}	Coherence time	s	393
ω	Angular frequency	(radian) s^{-1}	382
ψ	Energy fluence rate	$W\,m^{-2}$	405
Ψ	Energy fluence	$J\,m^{-2}$	405
Φ	Particle fluence	m^{-2}	388
Ω	Solid angle	sr	388

Problems

Section 14.1

Problem 1. The velocity of light c depends on the parameters ϵ_0 and μ_0. Use dimensional analysis to find what the dependence must be. Insert numerical values to obtain c.

Problem 2. An einstein is 1 mol of photons. Derive an expression for the energy in an einstein as a function of wavelength. Express the answer in kilocalories and the wavelength λ in nanometers.

Section 14.3

Problem 3. Use Eq. 14.8 to derive Eq. 14.9.

Problem 4. (a) Starting with Eq. 14.8, derive a formula for the hydrogen atom spectrum in the form

$$\frac{1}{\lambda} = R\left[\frac{1}{n^2} - \frac{1}{m^2}\right],$$

where n and m are integers. R is called the *Rydberg constant*. Find an expression for R in terms of fundamental constants.

(b) Verify that the wavelengths of the spectral lines a–d at the top of Fig. 14.3 are consistent with the energy transitions shown at the bottom of the figure.

Problem 5. The Lyman series, part of the spectrum of hydrogen, is shown at the top of Fig. 14.3 as the line labeled *a* and the band of lines to the left of that line. Create a figure like Fig. 14.3, but which shows a detailed view of the Lyman series. Let the wavelength scale at the top of your figure range from 0 to 150 nm, as opposed to 0–2 μm in Fig. 14.3. Also include an energy level drawing like at the bottom of Fig. 14.3 and indicate which transitions correspond to which lines in the Lyman spectrum. Indicate the shortest possible wavelength in the Lyman spectrum, show what transition that wavelength corresponds to, and determine how this wavelength is related to the Rydberg constant.

Problem 6. The left side of Fig. 14.1 shows the emission of a photon during a transition from an initial state with energy E_i to a final one with energy E_f. Usually the Boltzmann factor ensures that the population of the initial state is less than the final state. In some cases however, when the initial state is *metastable*, one can create a *population inversion*. Photons with energy $h\nu$ corresponding to the energy difference $E_i - E_f$ can produce *stimulated emission* of other photons with the same energy, a type of positive feedback. Lasers work on this principle. Suppose a laser is made using two states having an energy difference of 1.79 eV. What is the wavelength of the output light? What color does this correspond to? Lasers have many uses in medicine (Peng et al. 2008).

Section 14.4

Problem 7. Estimate $\hbar^2/2I$ for an HCl molecule. What would the spacing of rotational levels be?

Problem 8. An inulin molecule has a molecular weight of 4000 dalton (that is, 1 mol has a mass of 4000 g). Assume that it is spherical with a radius of 1.2 nm. What is the angular frequency ω of a photon absorbed when its rotational quantum number changes from 10 to 11? The moment of inertia of a sphere rotating about an axis through its center is $I = (2/5)mR^2$.

Problem 9. The rotational spectrum of HCl contains lines at 60.4, 69.0, 80.4, 96.4, and 120.4 μm. What is the moment of inertia of an HCl molecule?

Problem 10. Consider a combined rotational–vibrational transition for which r goes from 1 to 0 while v goes from v to $(v - 1)$. Find the frequencies of the photons emitted in terms of the moment of inertia of the molecule I, the angular frequency of vibration of the atoms in the molecule ω, and the quantum number v.

Problem 11. A rotating molecule emits photons when the rotational quantum number changes by 1. Find the ratio of the angular frequency of the photons, ω_{phot}, to the angular frequency of rotation of the molecule, ω_{rot}, as a function of the rotational quantum number r.

Section 14.5

Problem 12. A beam with 200 particles per square centimeter passes by an atom. The particles are uniformly and randomly distributed in the area of the beam.

(a) Fifty particles are scattered. What is the total scattering cross section?

(b) Ten particles are scattered in a cone of 0.1 sr solid angle about a particular direction. What is the differential cross section in $\text{m}^2\ \text{sr}^{-1}$?

Problem 13. The differential scattering cross section for a beam of x-ray photons of a certain energy from carbon at an angle θ is $50 \times 10^{-30}\ \text{m}^2\ \text{sr}^{-1}$. A beam of 10^5 photons strikes a pure carbon target of thickness 0.3 cm. The density of carbon is $2\ \text{g cm}^{-3}$, and the atomic weight is 12. The detector is a circle of 1 cm radius located 20 cm from the target. How many scattered photons enter the detector?

Problem 14. Photochemists often use the *extinction coefficient* e, defined by $\mu_a = eC$, where C is the concentration in moles per liter. This assumes the substance being measured is dissolved in a completely transparent solvent.

(a) What are the units of the extinction coefficient?

(b) What is the conversion between the extinction coefficient and the absorption cross section?

Problem 15. Suppose that the absorption coefficient in some biological substance is 5 m^{-1}. Make the very crude assumption that the substance has the density of water and a molecular weight of 18. What is the absorption cross section?
Problem 16. For blue light ($\lambda = 470$ nm), the attenuation coefficient in air is about 2×10^{-5} m^{-1}, and the attenuation coefficient in pure water is about 5×10^{-3} m^{-1}. Calculate the distance that blue light must pass through air and water before the intensity is reduced to 1% of the original intensity. Compare these distances to the thickness of the atmosphere and the depth of the ocean. Do you think that aquatic plants can use photosynthesis effectively at the bottom of the ocean? For more on the differences between the optical properties of air and water, see Denny (1993).

Section 14.6

Problem 17. (a) Find the slope of $\log R$ versus t in Eq. 14.30. What is its value for large times?

(b) What can be determined from the time when R has its maximum value? (Hint: R has a maximum when $\log R$ has a maximum.)
Problem 18. The result of one set of infrared measurements in human calf (leg) muscle gave a total scattering coefficient $\mu_s = 8.3$ cm^{-1} and an absorption coefficient $\mu_a = 0.176$ cm^{-1}.

(a) What fraction of the photons have not scattered in passing through a layer that is 8 μm thick? (This corresponds roughly to the size of a cell.)
(b) On average, how many scattering events take place for each absorption event?
(c) What is the cross section for scattering per molecule? For this estimate, assume the muscle consists entirely of water, with molecular weight 18 and density 10^3 kg m^{-3}.

Problem 19. Consider light with fluence rate φ_0 continuously and uniformly irradiating a half-infinite slab of tissue having an absorption coefficient μ_a and a reduced scattering coefficient μ_s'. Divide the photons into two types: the incident ballistic photons that have not yet interacted with the tissue, and the diffuse photons undergoing multiple scattering. The diffuse photon fluence rate, φ, is governed by the steady state limit of the photon diffusion equation (Eq. 14.27). The source of diffuse photons is the scattering of ballistic photons, so the source term in Eq. 14.27 is $s = \mu_s' \exp(-z/\lambda_{\text{unatten}})$, where z is the depth below the tissue surface. At the surface ($z = 0$), the diffuse photons obey the boundary condition $\varphi = 2Dd\varphi/dz$.[17]

(a) Derive an analytical expression for the diffuse photon fluence rate in the tissue, $\varphi(z)$.
(b) Plot $\varphi(z)$ versus z for $\mu_a = 0.08$ mm^{-1} and $\mu_s' = 4$ mm^{-1}.
(c) Evaluate λ_{unatten} and λ_{diffuse} for these parameters.

Section 14.7

Problem 20. Carry out the averages leading to Eq. 14.31.
Problem 21. If yellow light from a source has a coherence time of 10^{-8} s, how many cycles are there in the wave?
Problem 22. What coherence time is needed for a spatial resolution of 1 μm?
Problem 23. An infrared transition involves an energy of 0.1 eV. What are the corresponding frequency and wavelength? If the Raman effect is observed with light at 550 nm, what will be the frequencies and wavelengths of each Raman line?
Problem 24. A Raman spectrum has a line at 500 nm with subsidiary lines at 400 and 667 nm. What is the wavelength of the corresponding infrared line?

Section 14.8

Problem 25. Sodium is introduced into a flame at 2500 K. What fraction of the atoms are in their first excited state? In their ground state? (Remember that the characteristic sodium line is yellow.) If the flame temperature changes by 10 K, what is the fractional change in the population of each state? Which method of measuring sodium concentration is more stable to changes in flame temperature: measuring the intensity of an emitted line or measuring the amount of absorption?
Problem 26. (a) Show that the maximum of the thermal radiation function $W_\lambda(\lambda, T)$ occurs at a wavelength such that $e^x(5 - x) = 5$, where $x = hc/(\lambda_{\max} k_B T)$. Verify that $x = 4.9651$ is a solution of this transcendental equation, so that

$$T\lambda_{\max} = \frac{hc}{4.9651 k_B}.$$

(b) Similarly, show that

$$\frac{\nu_{\max}}{T} = \frac{2.82144 k_B}{h}$$

and that $\lambda_{\max}\nu_{\max} = 0.57c$.
Problem 27. Let $W_\nu(\nu) = A\nu(\nu_0 - \nu)$ for $\nu < \nu_0$, and $W_\nu(\nu) = 0$ otherwise.

(a) Plot $W_\nu(\nu)$ versus ν.
(b) Calculate the frequency corresponding to the maximum of $W_\nu(\nu)$, called $\nu_{\max}$.

[17] The derivation of this boundary condition is found in Haskell et al. (1994). See also Roth (2008).

(c) Let $\lambda_0 = c/\nu_0$ and $\lambda_{max} = c/\nu_{max}$. Write λ_{max} in terms of λ_0.
(d) Integrate $W_\nu(\nu)$ over all ν to find W_{tot}.
(e) Use Eqs. 14.36 and 14.37 to calculate $W_\lambda(\lambda)$.
(f) Plot $W_\lambda(\lambda)$ versus λ.
(g) Calculate the wavelength corresponding to the maximum of $W_\lambda(\lambda)$, called λ^*_{max}, in terms of λ_0.
(h) Compare λ_{max} and λ^*_{max}. Are they the same or different? If λ_0 is 400 nm, calculate λ_{max} and λ^*_{max}. What part of the electromagnetic spectrum is each of these in?
(i) Integrate $W_\lambda(\lambda)$ over all λ to find W^*_{tot}. Compare W_{tot} and W^*_{tot}. Are they the same or different?

Problem 28. Integrate Eq. 14.33 over all wavelengths to obtain the Stefan–Boltzmann law, Eq. 14.34. You will need the integral

$$\int_0^\infty \frac{x^3 dx}{e^x - 1} = \frac{\pi^4}{15}.$$

Problem 29. Two parallel surfaces of area S have unit emissivity and are at temperatures T_1 and T_2 [$T_1 > T_2$, panel (a)]. They are large compared to their separation, so that all radiation emitted by one surface strikes the other. Assume that radiation is emitted and absorbed only by the two surfaces that face each other. Let P_0 be the energy lost per unit time by body 1. A new sheet of perfectly absorbing material is introduced between bodies 1 and 2, as shown in panel (b). It comes to equilibrium temperature T. Let P be the net energy lost by surface 1 in this case. Find P/P_0 in terms of T_1 and T_2.

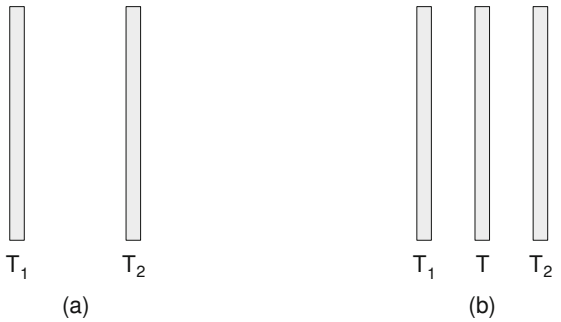

Problem 30. The sun has a radius of 6.9×10^8 m. The earth is 149.5×10^9 m from the sun. Treat the sun as a thermal radiator at 5800 K and calculate the energy from the sun per unit area per unit time striking the upper atmosphere of the earth (the solar constant). State the result in W m^{-2} and cal cm^{-2} min^{-1}.

Problem 31. If all the energy received by the earth from the sun is lost as thermal radiation (a poor assumption because a significant amount is reflected from cloud cover), what is the equilibrium temperature of the earth?

Section 14.9

Problem 32. Show that an approximation to Eq. 14.41 for small temperature differences is $w_{tot} = SK_{rad}(T - T_s)$. Deduce the value of K_{rad} at body temperature. Hint: Factor $T^4 - T_s^4 = (T - T_s)(\cdots)$. You should get $K_{rad} = 6.76$ W m^{-2} K^{-1}.

Problem 33. What fractional change in $W_\lambda(\lambda, T)$ for thermal radiation from the human body results when there is a temperature change of 1 K at 5 μm? 9 μm? 15 μm?

Section 14.10

Problem 34. (a) Suppose that the threshold for erythema caused by sunlight with $\lambda = 300$ nm is 30 J m^{-2}. Does this suggest that the result is thermal (an excessive temperature increase) or something else, like the photoelectric effect or photodissociation? Make some reasonable assumptions to estimate the temperature rise.

(b) The energy in sunlight at all wavelengths reaching the earth is 2 cal cm^{-2} min^{-1}. Suppose that the total body area exposed is 0.6 m^2. What would be the temperature rise per minute for a 60 kg person if there were no heat-loss mechanisms? Compare the rate of energy absorption to the basal metabolic rate, about 100 W.

Problem 35. Suppose that the energy fluence rate of a parallel beam of ultraviolet light that has passed through thickness x of solution is given by $\psi = \psi_0 e^{-\mu_a x}$. (Scattering is ignored.) The absorption coefficient μ_a is related to the concentration C (molecules cm^{-3}) of the absorbing molecules in the solution by $\mu_a = eC$. Biophysicists working with ultraviolet light define the dose rate to be the power absorbed per molecule of absorber. (This is a different definition of dose than is used in Chap. 15.) Calculate the dose rate for a thin layer ($\mu_a x \ll 1$).

Problem 36. A beam of photons passes through a monatomic gas of molecular weight A and absorption cross section σ. Ignore scattering. The gas obeys the ideal gas law, $pV = Nk_BT$.
(a) Find the attenuation coefficient in terms of σ, p, and any other necessary variables.
(b) Generalize the result to a mixture of several gases, each with cross section σ_i, partial pressure p_i, and N_i molecules.

Problem 37. The attenuation of a beam of photons in a gas of pressure p is given by $d\Phi = -\Phi(\sigma p/k_BT)\,dx$, where σ is the cross section, k_B the Boltzmann constant, T the absolute temperature, and x the path length. Suppose that the pressure is given as a function of altitude y by $p = p_0 e^{-mgy/k_BT}$. What is the total attenuation by the entire atmosphere?

Problem 38. Consider a beam of photons incident on the atmosphere from directly overhead. The atmosphere contains several species of molecules, each with partial pressure p_i. The absorption coefficient is $\mu_a = (1/k_B T) \sum_i \sigma_i p_i$. If each constituent of the atmosphere varies with height y as $p_i(y) = p_{0i} \exp(-m_i g y / k_B T)$, show that the fluence rate striking the earth is given by an expression of the form $e^{-\alpha}$ and find α.

Section 14.11

Problem 39. Consider a tissue with a specific heat of 3.6 J kg^{-1} K^{-1}, a density of 1000 kg m^{-3}, and a thermal conductivity of 0.5 W m^{-1} K^{-1}. Assume the specific heat of blood is the same, and that the tissue perfusion is 4.17×10^{-6} m^3 kg^{-1} s^{-1}. Find the thermal diffusivity, the time for the heat to flow 1 cm, and the thermal penetration depth.

Section 14.12

Problem 40. Suppose that a sphere radiates uniformly from its surface according to Lambert's cosine law: $L = L_0$. By considering area $dS = 2\pi r^2 \sin\theta \, d\theta$ on the surface of a sphere, find the power radiated per steradian in the direction of the z axis and the total power radiated.

Problem 41. Show that the exitance, total power per unit area radiated from a surface obeying Lambert's cosine law, is $W_r = \pi L_0$.

Problem 42. How many photons per second correspond to 1 lm at 555 nm for photopic vision? At 510 nm for scotopic vision?

Section 14.13

Problem 43. A person is nearsighted, and the relaxed eye focuses at a distance of 50 cm. What is the strength of the desired corrective lens in diopters?

Problem 44. What is the distance of closest vision for an average person with normal vision at age 20? Age 40? Age 60?

Problem 45. A person of age 40 is fitted with bifocals with a strength of +1 diopter more than the correction for distance vision. What are the closest and farthest distances of focus without the bifocal lens and with it? By the time the person is age 50, what are they with and without the same lens?

Problem 46. You can make a rough measurement of your own eye's properties. Tape a piece of paper with some pattern on it on the wall. Cover one eye. Move away from the wall until the pattern starts to blur. Measure the distance to the wall in meters. Calculate the vergence of the object, U. Assume that the F of your relaxed eye is 59 diopters. Calculate V for your eye. Now find the closest distance at which you can see the paper. Calculate the accommodation of your eye.

Problem 47. An object is placed 6 cm from a converging lens with a 5-cm focal length.

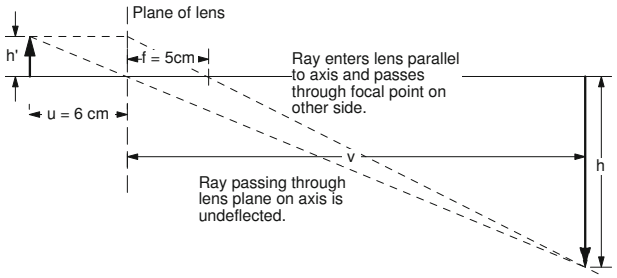

(a) Use the thin-lens equation (Eq. 14.64) to calculate the image distance.

(b) The magnification of the image is given by $m = -v/u$. (A negative magnification implies an inverted image.) What is the magnification for the image in part (a)? A value $|m| > 1$ implies a"magnified" image. This is how a slide projector works.

Problem 48. An object is placed 15 cm from a converging lens with a focal length of 20 cm.

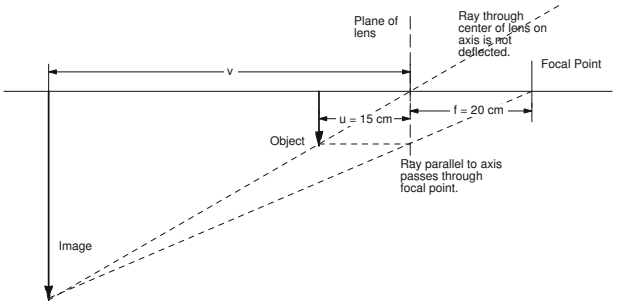

(a) Use the thin-lens equation (Eq. 14.64) to calculate the image distance. Your value should be negative, corresponding to a "virtual image".

(b) The magnification of the image is again given by $m = -v/u$. What is the magnification for the image in part (a)? This is how a magnifying glass works.

Problem 49. Combine the results of Problems 47 and 48. Consider two lenses, the first with focal length 5 cm and the second with focal length 20 cm, separated by 45 cm. The object is 6 cm in front of the first lens. The image from the first lens is the object for the second.

(a) Calculate the image distance and magnification of the image created by the first lens (called the objective).

(b) Use the first image as the object for the second lens (called the eyepiece), and calculate the image distance and magnification of the second image.

(c) The total magnification is the product of the magnifications of the objective and eyepiece. What is the total magnification? This is how the compound microscope works. The objective lens acts like a slide projector, and the eyepiece acts like a magnifying glass. Very large total magnifications can be obtained when the object is just to the left of the focal point of the objective, and the first image is just to the right of the focal point of the eyepiece.

Problem 50. Snell's law, $n_1 \sin\theta_1 = n_2 \sin\theta_2$, gives an interesting result if light passes from a medium with a higher index of refraction to one with a lower index of refraction, $n_1 > n_2$. Assume light passes from glass ($n_1 = 1.5$) to air ($n_2 = 1.0$).

(a) If θ_1 is 30°, what is θ_2?
(b) If θ_1 is 40°, what is θ_2?
(c) If θ_1 is 50°, what is θ_2?
This is really a tricky question, because for θ_1 greater than some *critical angle*, θ_c, θ_2 exceeds 90°, and light cannot pass into the second medium. Instead all the light is reflected and remains within the first medium.
(d) Calculate the critical angle for *total internal reflection* from glass to air.

Total internal reflection allows thin glass fibers to act as fiberoptic "light pipes," which can be used to transmit signals. Bundles of such optical fibers are used in endoscopes to see inside the body.

Problem 51. Table 14.7 shows that most of the converging power of the eye occurs at the air-cornea interface. When a person is under water, this must be supplied by the water-cornea surface. The index of refraction of the cornea is closer to that of water than to that of air. What are the implications for seeing under water? What are the implications for the vision of aquatic animals? (For more information on the difference between the eyes of aquatic and terrestrial animals, see Denny 1993.)

Section 14.14

Problem 52. How many photons per 0.1 s enter the eye from a 100 W light bulb 1000 ft away? Assume the pupil is 6 mm in diameter. How far away can a 100 W bulb be seen if there is no absorption in the atmosphere? Use a luminous efficiency of 17 lm W^{-1} and then assume an equivalent light source at 555 nm.

Problem 53. The table below shows the radiance of some extended sources. Without worrying about obliquity factors (assume that all the light is at normal incidence), calculate the number of photons entering a receptive field of 0.17° diameter when the pupil diameter is 6 mm and the integration time is 0.1 s. Assume a conversion efficiency of 100 lm W^{-1} and then assume that all the photons are at 555 nm.

Source	Radiance (lm m^{-2} sr^{-1})
White paper in sunlight	25000
Clear sky	3200
Surface of the moon	2900
White paper in moonlight	0.03

Problem 54. A piece of paper is illuminated by dim light so that its radiance is 0.01 lm m^{-2} sr^{-1} in the direction of a camera. A camera lens 1 cm in diameter is 0.6 m from the paper. The sheet of paper is 10 × 10 cm. The shutter of the camera is open for 1 ms. Assume all the light is at 555 nm. How many photons from the paper enter the lens of the camera while the shutter is open?

Problem 55. If three or more photons must be absorbed by a visual receptor field for the observer to see a flash, what fraction of the flashes are seen if the average number of photons absorbed in a receptor field per flash is four?

Problem 56. Assume that an average of d photons are detected and that the photons are Poisson distributed. What must d be to detect a signal that is a 1% change in d, if the signal-to-noise ratio must be at least 5?

Problem 57. Suppose that the average number of photons striking a target during an exposure is m. The probability that x photons strike during a similar exposure is given by the Poisson distribution. What is the probability that an organism responds to an exposure of radiation in each of the following cases?

(a) The response of the organism requires that a single target within the organism be hit by two or more photons.
(b) The response of the organism requires that two targets within the organism each be struck by one or more photons during the exposure.

References

AAPM 57 (1996) Recommended nomenclature for physical quantities in medical applications of light. American Association of Physicists in Medicine (AAPM) Report No. 57. College Park, MD

Armstrong CM (2012) The truth about terahertz radiation. IEEE Spectr 49:36–41

Armstrong BK, Kricker A (2001) The epidemiology of UV induced skin cancer. J Photochem Photobiol B Biol 63:8–18

Barlow HB (1956) Retinal noise and absolute threshold. J Opt Soc Am 46:634–639

Barlow HB (1957) Incremental thresholds at low intensities considered as signal/noise discriminations. J Physiol 136:469–488

Barysch MJ, Hofbauer GF, Dummer R (2010) Vitamin D, ultraviolet exposure, and skin cancer in the elderly. Gerontology 56:410–413. doi:10.1159/000315119

Bergmanson JPG, Söderberg PG (1995) The significance of ultraviolet radiation for eye diseases. A review with comments on the efficacy of UV-blocking contact lenses. Ophthalmic Physiol Opt 15(2):83–91

Berne BJ, Pecora R (1976) Dynamic light scattering: with applications to chemistry, biology, and physics. Wiley, New York
Blume S (1993) Social process and the assessment of a new imaging technique. Intl J Technol Assess Health Care 9(3):335–345
Bramson MA (1968) Infrared radiation. Plenum, New York
Brezinski ME (2006) Optical coherence tomography. Elsevier, Amsterdam
Buka RL (2004) Sunscreens and insect repellents. Curr Opin Pediatr 16:378–384
Charman WN (2009) Optics of the eye. In: Bass M (ed) Handbook of optics, 3rd ed, Vol. III. McGraw-Hill, New York. (Sponsored by the Optical Society of America.)
Cornsweet TN (1970) Visual perception. Academic, New York
de Boer JF Srinivas SM Nelson JS Milner TE Ducros MG (2002) Polarization-sensitive optical coherence tomography. In: Bouma BE, Tearney GJ (eds) Handbook of optical coherence tomography. Marcel Dekker, New York, pp 274–298
Denny MW (1993) Air and water: the biology and physics of life's media. Princeton University Press, Princeton
Diem M (1993) Introduction to modern vibrational spectroscopy. Wiley, New York
Diffey BL (1991) Solar ultraviolet radiation effects on biological systems. Phys Med Biol 36(3):299–328
Diffey BL, Cheeseman J (1992) Sun protection with hats. Brit J Dermatol 127(1):10–12
Duderstadt JJ, Hamilton LJ (1976) Nuclear reactor analysis. Wiley, New York
Eisberg R, Resnick R (1985) Quantum physics of atoms, molecules, solids, nuclei and particles, 2nd ed. Wiley, New York
Esenaliev RO, Larin KV, Larina IV, Motamedi M (2001) Noninvasive monitoring of glucose concentration with optical coherence tomography. Opt Lett 26(13):992–994
Farmer J (1997) Blood oxygen measurement. In: Webster JG (ed) Design of pulse oximeters. Institute of Physics, Bristol
Fercher AF, Drexler W, Hitzenberger CK, Lasser T (2003) Optical coherence tomography: principles and applications. Rep Prog Phys 66:239–303
Fitzgerald AJ, Berry E, Zinovev NN, Walker GC, Smith MA, Chamberlain JM (2002) An introduction to medical imaging with coherent terahertz frequency radiation. Phys Med Biol 47:R67–R84
Fraden J (1991) Noncontact temperature measurements in medicine. In: Wise DL (ed) Bioinstrumentation and biosensors. Dekker, New York, pp 511–549
Gasiorowicz S (2003) Quantum physics, 3rd ed. Wiley, New York
Giasson CJ, Quesnel N-M, Boisjoly H (2005) The ABCs of ultraviolet-blocking contact lenses: an ocular panacea for ozone loss? Int Ophthalmol Clin 45(1):117–139
Greivenkamp JE, Schwiegerling J, Miller JM, Mellinger MD (1995) Visual acuity modeling using optical raytracing of schematic eyes. Am J Ophthalmol 120(2):227–240
Grossweiner L (1994) The science of phototherapy. CRC, Boca Raton
Hanlon EB, Manoharan R, Koo T-W, Shafer KE, Motz JT, Fitzmaurice M, Kramer JR, Itzkan I, Dasari RR, Feld MS (2000) Prospects for *in vivo* Raman spectroscopy. Phys Med Biol 45:R1–R59
Hao O-Y, Stanfield J, Cole C, Appa Y, Rigel D (2012) High-SPF sunscreens (SPF $\geq$ 70) may provide ultraviolet protection above minimal recommended levels by adequately compensating for lower sunscreen user application amounts Capsule Summary. J Am Acad Dermatol 67(6):1220–1227. doi:10.1016/j.jaad.2013.04.002
Halliday D, Resnick R, Krane KS (1992) Fundamentals of physics, 4th ed., extended edition, Vol. 2 . Wiley, p 1022
Haskell RC, Svassand LO, Tsay T-T, Feng T-C, McAdams MS, Tromberg BJ (1994) Boundary conditions for the diffusion equation in radiative transfer. J Opt Soc Am A 11(10):2727–2741
Heald MA (2003) Where is the "Wien peak"? Am J Phys 71(12):1322–1323
Hecht S, Shlaer S, Pirenne MH (1942) Energy, quanta, and vision. J Gen Physiol 25:819–840
Hielscher A, Jacques SL, Wang L, Tittel FK (1995) The influence of boundary conditions on the accuracy of diffusion theory in time-resolved reflectance spectroscopy of biological tissues. Phys Med Biol 40:1957–1975
Huang D, Swanson EA, Lin CP , Schuman JS, Stinson WG, Chang W, Hee MR, Flotte T, Gregory K, Puliafito CA, Fujimoto JG (1991) Optical coherence tomography. Science 254:1178–1181
Johnsen S (2011) The optics of life: a biologist's guide to light in nature. Princeton University Press, Princeton
Kevan PG, Chittka L, Dyer AG (2001) Limits to the salience of ultraviolet: lessons from colour vision in bees and birds. J Exp Biol 204:2571–2580
Kimlin MG, Parisi AV (1999) Ultraviolet radiation penetrating vehicle glass: a field based comparative study. Phys Med Biol 44:917–926
Kligman LH (1989) Photoaging: manifestations, prevention, and treatment. Clin Geriatr Med 5:235–251
Knobler R, Barr ML, Couriel DR, Ferrara JLM, French LE, Jaksch P, Reinisch W, Rook AH, Schwarz T, Greinix H (2009) Extracorporeal photopheresis: past, present, and future. J Am Acad Dermatol 61:652–665
Kripke ML (2003) The ABCs of sunscreen protection factors. J Invest Dermatol 121(1):vii–viii
Lahiri BB, Bagavathiappan S, Jayakumar T, Philip J (2012) Medical applications of infrared thermography: a review. Infrared Phys Technol 55:221–235
Lazovich D, Vogel RI, Berwick M, Weinstock MA, Anderson KE, Warshaw EM (2010) Indoor tanning and risk of melanoma: a case-control study in a highly exposed population. Cancer Epidemiol Biomarkers Prev 19(6):1557–1568
Liu H, Boas DA, Zhang Y, Yodh AG, Chance B (1995) Determination of optical properties and blood oxygenation in tissue using continuous NIR light. Phys Med Biol 40:1983–1993
MacNeill BD, Lowe HC, Takano M, Fuster V, Jang I-K (2003) Intravascular modalities for detection of vulnerable plaque. Arterioscler Thromb Vasc Biol 23:1333–1342
Madronich S (1993) The atmosphere and UV-B radiation at ground level. In: Young AR et al. (eds) Environmental UV photobiology. Plenum, New York, pp 1–39
McDonagh AF (1985) Light effects on transport and excretion of bilirubin in newborns. Ann NY Acad Sci 453:65–72
Moyal DD, Fourtanier AM (2002) Effects of UVA radiation on an established immune response in humans and sunscreen efficacy. Exp Dermatol 11(Suppl. 1):28–32
Murphy MR, Oellrich RG (1990) A new method of phototherapy: nursing perspectives. J Perinatol 10(3):249–251
Nickell S, Hermann M, Essenpreis M, Farrell TJ, Krämer U, Patterson MS (2000) Anisotropy of light propagation in human skin. Phys Med Biol 45:2873–2886
O'Sullivan N, Tait C (2014) Tanning bed and nail lamp use and the risk of cutaneous malignancy: a review of the literature. Australas J Dermatol 55:99–106. doi:10.1111/ajd.12145
Patterson MS, Chance B, Wilson BC (1989) Time resolved reflectance and transmittance for the non-invasive measurement of tissue optical properties. Appl Opt 28(12):2331–2336
Peng Q, Juzeniene A, Chen J, Svaassand LO, Warloe T, Giercksky K-E, Moan J (2008) Lasers in medicine. Rep Prog Phys 71:056701. doi:10.1088/0034-4885/71/5/056701
Pillsbury DM, Heaton CL (1980) A manual of dermatology, 2nd ed. Saunders, Philadelphia, p 5
Pogue BW, Patterson MS (1994) Frequency-domain optical absorption spectroscopy of finite tissue volumes using diffusion theory. Phys Med Biol 39:1157–1180
Rieke F, Baylor DA (1998) Single-photon detection by rod cells of the retina. Rev Mod Phys 70(3):1027–1036

Rodieck RW (1998) The first steps in seeing. Sunderland, Sinauer
Rose A (1973) Vision: human and electronic. New York, Plenum
Roth BJ (2008) Photon density measured over a cut surface: implications for optical mapping of the heart. IEEE Trans Biomed Eng 55(8):2102–2104
Saint-Jalmes H, Lebec M, Beaurepaire E, Dubois A, Boccara AC (2002) Full-field optical coherence microscopy. In: Bouma BE, Tearney GJ (eds) Handbook of optical coherence tomography. Marcel Dekker, New York , pp 299–333
Sakitt B (1972) Counting every quantum. J Physiol (London) 223:131–150
Schmidt CW (2012) UV radiation and skin cancer: the science behind age restrictions for tanning beds. Environ Health Perspect 120(8):A308–A313
Schmitt JM (1999) Optical coherence tomography (OCT): a review. IEEE J Sel Top Quantum Electron 5:1205–1215
Schroeder DV (2000) An introduction to thermal physics. Addison Wesley Longman, San Francisco
Serway RA, Jewett JW (2013) Principles of physics, 5th ed. Brooks/Cole, Boston
Sevick EM, Chance B, Leigh J, Nioka S, Maris M (1991) Quantitation of time- and frequency-resolved optical spectra for the determination of tissue oxygenation. Analyt Biochem 195:330–351
Smye SW, Chamberlain JM, Fitzgerald AJ, Berry E (2001) The interaction between terahertz radiation and biological tissue. Phys Med Biol 46:R101–R112
Soffer BH, Lynch DK (1999) Some paradoxes, errors, and resolutions concerning spectral optimization of human vision. Am J Phys 67(11):946–953
Stark L, Theodoridis GC (1973) Information theory in physiology. In: Brown JHU, Gans DS (eds) Engineering principles in physiology, Vol. 1. Academic, New York , pp 13–31
Steketee J (1973) Spectral emissivity of skin and pericardium. Phys Med Biol 18:686–694
Stern RS (2007) Psoralen and ultraviolet—A therapy for psoriasis. N Engl J Med 357:682–690
Teramura T, Mizuno M, Asano H, Naito N, Arakane K, Miyachi Y (2012) Relationship between sun-protection factor and application thickness in high-performance sunscreen: double application of sunscreen is recommended. Clin Exp Dermatol 37:904–908. doi:10.1111/j.1365-2230.2012.04388.x
Verheye S, Diamantopoulos L, Serruys PW, van Langenhove G (2002) Intravascular imaging of the vulnerable atherosclerotic plaque: spotlight on temperature measurement. J Cardiovasc Risk 9:247–254
Vreugdenburg TD Willis CD Mundy L Hiller JE (2013). A systematic review of elastography, electrical impedance scanning, and digital infrared thermography for breast cancer screening and diagnosis. Breast Cancer Res Treat 137:665–676. doi:10.1007/s10549-012-2393-x
Webster JG (1997) Design of pulse oximeters. Institute of Physics Publishers, Bristol
Wieben O (1997) Light absorbance in pulse oximetry. In: Webster JG (ed) Design of pulse oximeters. Institute of Physics Publishers, Bristol
Wilson BC, Patterson MS (2008) The physics, biophysics and technology of photodynamic therapy. Phys Med Biol 53:R61–R109
Yamashita Y, Maki A, Koizumi H (2001) Wavelength dependence of the precision of noninvasive optical measurement of oxy-, deoxy-, and total-hemoglobin concentration. Med Phys 28(6):1108–1114
Yasuno Y, Makita S, Sutoh Y, Itoh M, Yatagai T (2002) Birefringence imaging of human skin by polarization-sensitive spectral interferometric optical coherence tomography. Opt Lett 27(20):1803–1805
Yazdanfar S, Rollins AM, Izatt JA. Imaging and velocimetry of the human retinal circulation with color Doppler optical coherence tomography. Opt Lett 25(19):1448–1450
Yodh A, Chance B (1995) Spectroscopy and imaging with diffusing light. Phys Today 48(3):34–41
Zalewski EF (2009) Radiometry and photometry In: Bass M (ed) Handbook of Optics, 3rd ed. McGraw-Hill, New York. (Sponsored by the Optical Society of America)
Zhang X-C (2002) Terahertz wave imaging: horizons and hurdles. Phys Med Biol 47:3667–3677
Zhu TC, Finlay JC (2008) The role of photodynamic therapy (PDT) physics. Med Phys 35:3127–3126